

Catalytic Hydrodefluorination of Aromatic Fluorocarbons by Ruthenium N-Heterocyclic Carbene Complexes

Steven P. Reade, Mary F. Mahon, and Michael K. Whittlesey*

Department of Chemistry, University of Bath, Claverton Down, Bath BA2 7AY, U.K.

Received August 18, 2008; E-mail: chsmkw@bath.ac.uk

Abstract: The catalytic hydrodefluorination (HDF) of hexafluorobenzene, pentafluorobenzene, and pentafluoropyridine with alkylsilanes is catalyzed by the ruthenium N-heterocyclic carbene (NHC) complexes Ru(NHC)(PPh₃)₂(CO)H₂ (NHC = SIMes (1,3-bis(2,4,6-trimethylphenyl)imidazolin-2-ylidene) **13**, SIPr (1,3-bis(2,6-diisopropylphenyl)imidazolin-2-ylidene) **14**, IPr (1,3-bis(2,6-diisopropylphenyl)imidazol-2-ylidene) **15**, IMes (1,3-bis(2,4,6-trimethylphenyl)imidazol-2-ylidene) **16**). Catalytic activity follows the order **15** > **13** > **16** > **14**, with **15** able to catalyze the HDF of C₆F₅H with Et₃SiH with a turnover number of up to 200 and a turnover frequency of up to 0.86 h⁻¹. The catalytic reactions reveal (i) a novel selectivity for substitution at the 2-position in C₆F₅H and C₅F₅N, (ii) formation of deuterated fluoroarene products when reactions are performed in C₆D₆ or C₆D₅CD₃, and (iii) a first-order dependence on [fluoroarene] and zero-order relationship with respect to [R₃SiH]. Mechanisms are proposed for HDF of C₆F₆ and C₆F₅H, the principal difference being that the latter occurs by initial C–H rather than C–F activation.

Introduction

The activation and functionalization of fluorocarbons represents a significant challenge due to the great strength of the C–F interaction.^{1,2} While there has been considerable progress in the stoichiometric cleavage of fluoroarenes,^{3–10} fluoroalkenes,^{8,11–13} and even fluoroalkanes,^{8,14,15} metal catalyzed transformations of C–F bonds remain relatively scarce.^{16–19} In 1994, Milstein and

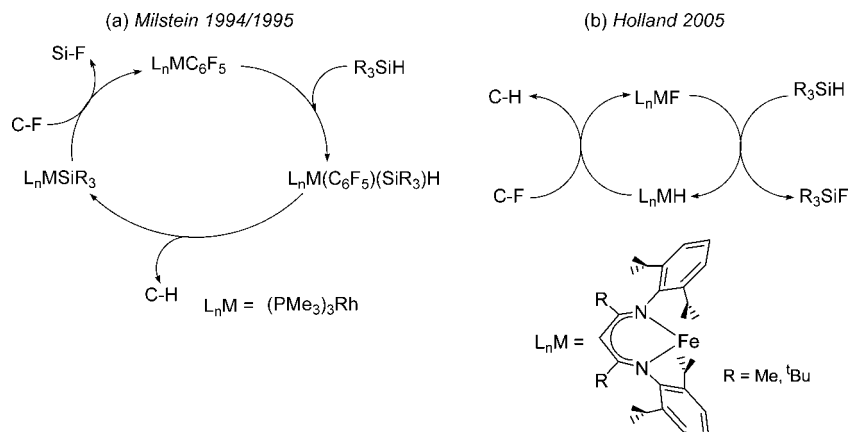
Aizenberg reported that hydrodefluorination (HDF) of C₆F₆ and C₆F₅H in the presence of R₃SiH (R' = Ph, OEt) was catalyzed by the Rh–silyl complex Rh(PMe₃)₃(SiR₃) (SiR₃ = SiPh₃, SiPhMe₂).²⁰ A year later, the same group showed that the pentafluorophenyl complex Rh(PMe₃)₃(C₆F₅) would also perform catalytic HDF in the presence of H₂.²¹ In both cases, the driving force for reaction involves the formation of a strong element–fluoride (E–F) bond, either R₃Si–F or HF, as summarized in Scheme 1a.

More recently, Holland and co-workers have reported the use of a β-diketiminato iron(II) fluoride species to catalyze HDF of perfluoroaromatics, as well as perfluoroalkenes, also in the

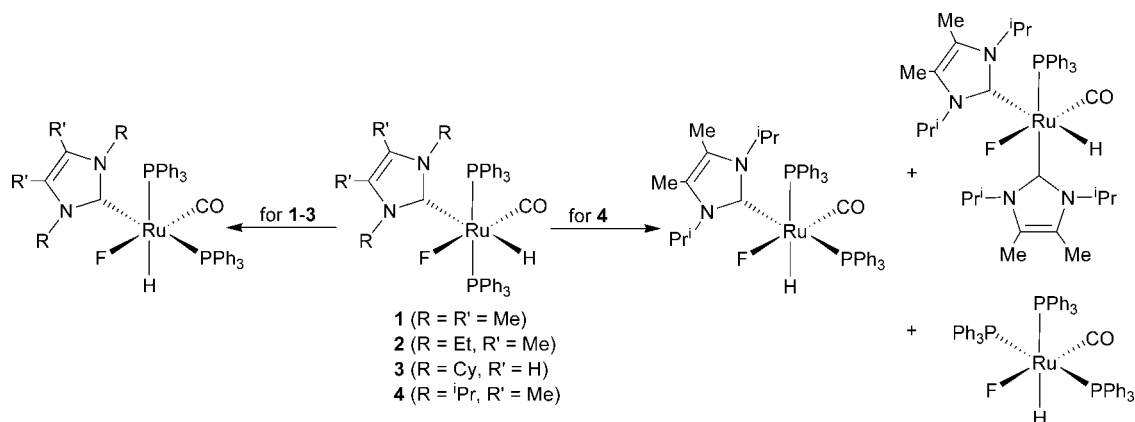
- (1) (a) Kiplinger, J. L.; Richmond, T. G.; Osterberg, C. E. *Chem. Rev.* **1994**, *94*, 373–431. (b) Burdeniuc, J.; Jedlicka, B.; Crabtree, R. H. *Chem. Ber./Recl.* **1997**, *130*, 145–154. (c) Richmond, T. G. *Top. Organomet. Chem.* **1999**, *3*, 243–269. (d) Richmond, T. G. *Angew. Chem., Int. Ed.* **2000**, *39*, 3241–3244. (e) Mazurek, U.; Schwarz, H. *Chem. Commun.* **2003**, 1321–1326. (f) Torrens, H. *Coord. Chem. Rev.* **2005**, *249*, 1957–1985.
- (2) Braun, T.; Perutz, R. N. In *Comprehensive Organometallic Chemistry III*; Crabtree, R. H., Mingos, D. M. P., Eds.; Elsevier: Oxford, 2007; Vol. 1, pp 725–758.
- (3) (a) Richmond, T. G.; Osterberg, C. E.; Arif, A. M. *J. Am. Chem. Soc.* **1987**, *109*, 8091–8092. (b) Jones, W. D.; Partridge, M. G.; Perutz, R. N. *J. Chem. Soc., Chem. Commun.* **1991**, 264–266. (c) Blum, O.; Frolow, F.; Milstein, D. *J. Chem. Soc., Chem. Commun.* **1991**, 258–259. (d) Hoffman, P.; Unfried, G. *Chem. Ber.* **1992**, *125*, 659–661. (e) Klahn, A. H.; Moore, M. F.; Perutz, R. N. *J. Chem. Soc., Chem. Commun.* **1992**, 1699–1701. (f) Edelbach, B. L.; Rahman, A. K. F.; Lachicotte, R. J.; Jones, W. D. *Organometallics* **1999**, *18*, 3170–3177. (g) Sladek, M. I.; Braun, T.; Neumann, B.; Stammler, H.-G. *J. Chem. Soc., Dalton Trans.* **2002**, 297–299. (h) Lindup, R. J.; Marder, T. B.; Perutz, R. N.; Whitwood, A. C. *Chem. Commun.* **2007**, 3664–3666.
- (4) Belt, S. T.; Helliwell, M.; Jones, W. D.; Partridge, M. G.; Perutz, R. N. *J. Am. Chem. Soc.* **1993**, *115*, 1429–1440.
- (5) (a) Cronin, L.; Higgitt, C. L.; Karch, R.; Perutz, R. N. *Organometallics* **1997**, *16*, 4920–4928. (b) Braun, T.; Foxon, S. P.; Perutz, R. N.; Walton, P. H. *Angew. Chem., Int. Ed.* **1999**, *38*, 3326–3329. (c) Braun, T.; Perutz, R. N. *Chem. Commun.* **2002**, 2749–2757.
- (6) Edelbach, B. L.; Jones, W. D. *J. Am. Chem. Soc.* **1997**, *119*, 7734–7742.
- (7) Reinhold, M.; McGrady, J. E.; Perutz, R. N. *J. Am. Chem. Soc.* **2004**, *126*, 5268–5276.
- (8) Jones, W. D. *Dalton Trans.* **2003**, 3991–3995.
- (9) Maron, L.; Werkema, E. L.; Perrin, L.; Eisenstein, O.; Andersen, R. A. *J. Am. Chem. Soc.* **2005**, *127*, 279–292.
- (10) Schaub, T.; Radius, U. *Chem.–Eur. J.* **2005**, *11*, 5024–5030.

- (11) (a) Watson, P. L.; Tulip, T. H.; Williams, I. *Organometallics* **1990**, *9*, 1999–2009. (b) Watson, L. A.; Yandulov, D. V.; Caulton, K. G. *J. Am. Chem. Soc.* **2001**, *123*, 603–611. (c) Ferrando-Miguel, G.; Gerard, H.; Eisenstein, O.; Caulton, K. G. *Inorg. Chem.* **2002**, *41*, 6440–6449. (d) Braun, T.; Noveski, D.; Neumann, B.; Stammler, H.-G. *Angew. Chem., Int. Ed.* **2002**, *41*, 2745–2749. (e) Noveski, D.; Braun, T.; Schulte, M.; Neumann, B.; Stammler, H.-G. *Dalton Trans.* **2003**, 4075–4083. (f) Clot, E.; Megret, C.; Kraft, B. M.; Eisenstein, O.; Jones, W. D. *J. Am. Chem. Soc.* **2004**, *126*, 5647–5653. (g) Huang, D. J.; Renkema, K. B.; Caulton, K. G. *Polyhedron* **2006**, *25*, 459–468. (h) Anderson, D. J.; McDonald, R.; Cowie, M. *Angew. Chem., Int. Ed.* **2007**, *46*, 3741–3744. (i) Rieth, R. D.; Brennessel, W. W.; Jones, W. D. *Eur. J. Inorg. Chem.* **2007**, 2839–2847.
- (12) Kirkham, M. S.; Mahon, M. F.; Whittlesey, M. K. *Chem. Commun.* **2001**, 813–814.
- (13) Kraft, B. M.; Jones, W. D. *J. Organomet. Chem.* **2002**, *658*, 132–140.
- (14) (a) Harrison, R. G.; Richmond, T. G. *J. Am. Chem. Soc.* **1993**, *115*, 5303–5304. (b) Bennett, B. K.; Harrison, R. G.; Richmond, T. G. *J. Am. Chem. Soc.* **1994**, *116*, 11165–11166. (c) Burdeniuc, J.; Crabtree, R. H. *Organometallics* **1998**, *17*, 1582–1586. (d) Kraft, B. M.; Lachicotte, R. J.; Jones, W. D. *J. Am. Chem. Soc.* **2000**, *122*, 8559–8560. (e) Werkema, E. L.; Messines, E.; Perrin, L.; Maron, L.; Eisenstein, O.; Andersen, R. A. *J. Am. Chem. Soc.* **2005**, *127*, 7781–7795.
- (15) Kraft, B. M.; Lachicotte, R. J.; Jones, W. D. *J. Am. Chem. Soc.* **2001**, *123*, 10973–10979.
- (16) Kiplinger, J. L.; Richmond, T. G. *J. Am. Chem. Soc.* **1996**, *118*, 1805–1806.

Scheme 1



Scheme 2



presence of silanes as the reductant (Scheme 1b).²² Intriguingly, and in contrast to the rhodium chemistry, the iron hydride species furnished by reaction of the iron fluoride with R_3SiH showed no evidence for direct C–F bond activation in the

absence of silane, a factor which has prevented the mechanism of catalysis being fully elucidated. In practical terms, both the Rh and Fe systems suffer disadvantages, in the need for either forcing conditions ($Rh(PMe_3)_3(C_6F_5)$ required the presence of ca. 6 atm of H_2 and 10 equiv of Et_3N (as a trap for released HF) at 373 K) or high catalyst loadings (20 mol% in the case of the Fe system). Both of these factors, along with higher catalytic activity, need to be addressed if more viable catalytic C–F functionalization is to be realized.

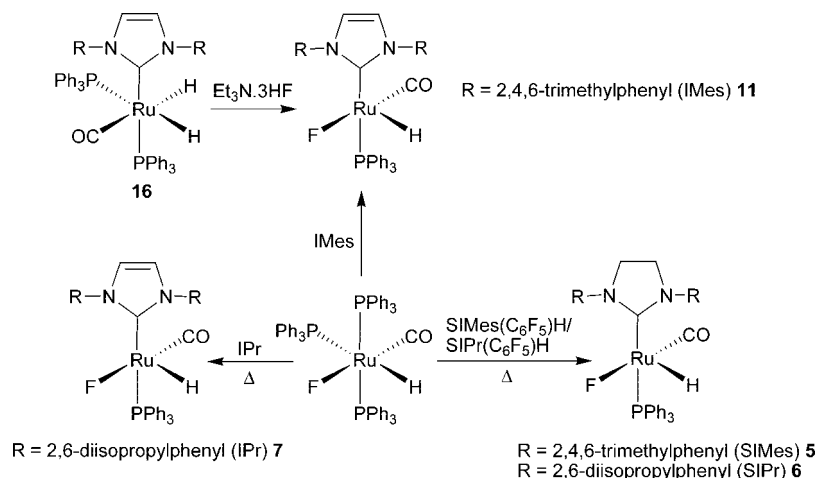
We recently reported the synthesis and reactivity of a series of N-heterocyclic carbene (NHC) ruthenium fluoride complexes $Ru(NHC)(PPh_3)_2(CO)HF$ containing the N-alkyl substituted NHCs IME_4 , IET_2Me_2 , ICy , and $I^iPr_2Me_2$ (complexes 1–4, Scheme 2).²³ These complexes, which can be formed quite easily and in good yield by addition of the free carbenes to $Ru(PPh_3)_3(CO)HF$, proved to be unstable in solution, isomerizing to the corresponding *cis*-phosphine isomers over a period of days at room temperature. In the case of 4, isomerization was also accompanied by disproportionation.

While reactivity studies on 1–4 were largely precluded by their willingness to isomerize/disproportionate, we found that for the most stable of them, the N-methyl species 1, the addition of Et_3SiH at room temperature afforded the dihydride complex $Ru(IME_4)(PPh_3)_2(CO)H_2$ and Et_3SiF . Given that $Ru(II)$ hydride complexes have been shown to activate C–F bonds under very

- (17) (a) Ishii, Y.; Chatani, N.; Yorimitsu, S.; Murai, S. *Chem. Lett.* **1998**, 157–158. (b) Young, R. J., Jr.; Grushin, V. V. *Organometallics* **1999**, *18*, 294–296. (c) Böhm, V. P. W.; Weskamp, T.; Gstöttmayr, C. W. K.; Herrmann, W. A. *Angew. Chem., Int. Ed.* **2001**, *40*, 3387–3389. (d) Braun, T.; Perutz, R. N.; Sladek, M. I. *Chem. Commun.* **2001**, 2254–2255. (e) Desmarets, C.; Kuhl, S.; Schneider, R.; Fort, Y. *Organometallics* **2002**, *21*, 1554–1559. (f) Kuhl, S.; Schneider, R.; Fort, Y. *Adv. Synth. Catal.* **2003**, *345*, 341–344. (g) Renkema, K. B.; Werner-Zwanziger, U.; Pagel, M. D.; Caulton, K. G. *J. Mol. Catal. A: Chem.* **2004**, *224*, 125–131. (h) Fuchibe, K.; Akiyama, T. *J. Am. Chem. Soc.* **2006**, *128*, 1434–1435. (i) Peterson, A. A.; McNeil, K. *Organometallics* **2006**, *25*, 4938–4940. (j) Braun, T.; Wehmeier, F.; Altenhöner, K. *Angew. Chem., Int. Ed.* **2007**, *46*, 5321–5324. (k) Fuchibe, K.; Ohshima, Y.; Mitomi, K.; Akiyama, T. *J. Fluorine Chem.* **2007**, *128*, 1158–1167.
- (18) Schaub, T.; Backes, M.; Radius, U. *J. Am. Chem. Soc.* **2006**, *128*, 15964–15965.
- (19) For other catalytic transformations involving C–F cleavage, see: (a) Terao, J.; Ikumi, A.; Kuniyasu, H.; Kambe, N. *J. Am. Chem. Soc.* **2003**, *125*, 5646–5647. (b) Terao, J.; Watabe, H.; Kambe, N. *J. Am. Chem. Soc.* **2005**, *127*, 3656–3657. (c) Scott, V. J.; Çelenigil-Çetin, R.; Ozerov, O. V. *J. Am. Chem. Soc.* **2005**, *127*, 2852–2853. (d) Panisch, R.; Bolte, M.; Müller, T. *J. Am. Chem. Soc.* **2006**, *128*, 9676–9682. (e) Klahn, M.; Fischer, C.; Spannenberg, A.; Rosenthal, U.; Krossing, I. *Tetrahedron Lett.* **2007**, *48*, 8900–8903. (f) Douvris, C.; Ozerov, O. V. *Science* **2008**, *321*, 1188–1190.
- (20) Aizenberg, M.; Milstein, D. *Science* **1994**, *265*, 359–361.
- (21) Aizenberg, M.; Milstein, D. *J. Am. Chem. Soc.* **1995**, *117*, 8674–8675.
- (22) Vela, J.; Smith, J. M.; Yu, Y.; Ketterer, N. A.; Flaschenriem, C. J.; Lachicotte, R. J.; Holland, P. L. *J. Am. Chem. Soc.* **2005**, *127*, 7857–7870.

- (23) Reade, S. P.; Nama, D.; Mahon, M. F.; Pregosin, P. S.; Whittlesey, M. K. *Organometallics* **2007**, *26*, 3484–3491.

Scheme 3



mild conditions,^{12,24} this suggested to us that if isomerization/disproportionation could be prevented, the facile interconversion of $\text{Ru}(\text{NHC})(\text{PPh}_3)_x(\text{CO})\text{HF}/\text{Ru}(\text{NHC})(\text{PPh}_3)_x(\text{CO})\text{H}_2$ ($x = 1, 2$) complexes might allow the design of a new catalytic system for C–F functionalization.

We now report that the use of N-aryl substituted NHCs affords a ruthenium system which catalyzes HDF of aromatic fluorocarbons. The isolation of both Ru hydride fluoride and dihydride complexes has allowed a mechanistic investigation of the reaction to be undertaken and revealed a number of unique features, particularly an unusual regioselectivity in the HDF products.

Results and Discussion

Synthesis and Characterization of $\text{Ru}(\text{NHC})(\text{PPh}_3)_x(\text{CO})\text{HF}$ ($x = 1, 2$). The coordinatively unsaturated complexes $\text{Ru}(\text{NHC})(\text{PPh}_3)(\text{CO})\text{HF}$ (NHC = SIMes **5**, SIPr **6**, IPr **7**; see Scheme 3 for structures of NHCs) were formed upon reaction of $\text{Ru}(\text{PPh}_3)_3(\text{CO})\text{HF}$ with the pentafluorobenzene adducts $\text{SIMes}(\text{C}_6\text{F}_5)\text{H}$ and $\text{SIPr}(\text{C}_6\text{F}_5)\text{H}$, or the free carbene IPr, at elevated temperatures.^{25,26} While the formation of the saturated carbene complex **5** was complete within 2.5 h at 343 K, more forcing conditions were needed for reaction of the bulkier 2,6-diisopropylphenyl substituted ligands (**6**: 393 K, 16 h; **7**: 363 K, 6 h).

The SIMes complex **5** was isolated from benzene/hexane and displayed NMR features expected for a five-coordinate $\text{Ru}(\text{NHC})(\text{PPh}_3)(\text{CO})\text{HF}$ structure, with a low frequency doublet hydride signal ($\delta -23.4$, $J_{\text{HP}} = 24$ Hz) and a doublet phosphorus resonance ($J_{\text{PF}} = 27$ Hz). The Ru–F signal appeared as a broad singlet at $\delta -215.8$,^{27–29} although the 27 Hz J_{FP} splitting was

resolved upon addition of Me_3SiCF_3 or CsF or upon redissolving crystalline **5**, suggesting that the broadening results from traces of adventitious moisture.³⁰ Both **6** and **7** proved to be highly hexane soluble and thus could not be completely separated from the PPh_3 produced in the substitution reaction.^{31,32} Consequently, their room temperature ^1H , ^{31}P , and ^{19}F spectra displayed Ru–H, PPh_3 , and Ru–F resonances which appeared (at best) as only poorly resolved doublets, suggestive of some interaction between the metal center and the residual phosphine. Upon cooling toluene solutions of both complexes to 214 K, a new set of hydride signals (with doublet of doublet multiplicity) appeared in each case at ca. $\delta -6$ in a 1:2.2 (**6**) and 1:0.2 (**7**) ratio with the starting material. A new, broad, low frequency ^{19}F signal was also apparent at ca. $\delta -360$ in each sample. The spectra are consistent with the appearance of the 18-electron bis-phosphine complexes $\text{Ru}(\text{SIPr})(\text{PPh}_3)_2(\text{CO})\text{HF}$ (**9**) and $\text{Ru}(\text{IPr})(\text{PPh}_3)_2(\text{CO})\text{HF}$ (**10**). NMR spectra recorded at 200 K upon the addition of further PPh_3 (total of 2.6 equiv present in solution) revealed complete conversion of the IPr complex **7** to **10**, while, in the case of the SIPr species, a 1:1 mixture of **6** and **9** was produced. Dissolution of a crystallized sample of **5** in the presence of 2.6 equiv of PPh_3 also resulted in the complete formation to $\text{Ru}(\text{SIMes})(\text{PPh}_3)_2(\text{CO})\text{HF}$ (**8**) at 200 K.

The N-mesityl carbene complex $\text{Ru}(\text{IMes})(\text{PPh}_3)(\text{CO})\text{HF}$ (**11**) (IMes = 1,3-bis(2,4,6-trimethyl)phenylimidazol-2-ylidene) was formed by reaction of IMes with $\text{Ru}(\text{PPh}_3)_3(\text{CO})\text{HF}$, although both $\text{Ru}(\text{IMes})_2(\text{CO})\text{HF}$ ^{25b} and $\text{Ru}(\text{PPh}_3)_3(\text{CO})\text{H}_2$ were also

(24) Whittlesey, M. K.; Perutz, R. N.; Moore, M. F. *Chem. Commun.* **1996**, 787–788.

(25) There are relatively few examples of NHC metal fluoride complexes known. See refs 10, 18, and 23 along with: (a) Laitar, D. S.; Müller, P.; Gray, T. G.; Sadighi, J. P. *Organometallics* **2005**, *24*, 4503–4505. (b) Chatwin, S. L.; Davidson, M. G.; Doherty, C.; Donald, S. M.; Jassar, R. F. R.; Macgregor, S. A.; McIntyre, G. J.; Mahon, M. F.; Whittlesey, M. K. *Organometallics* **2006**, *25*, 99–110. (c) Nikiforov, G. B.; Roesky, H. W.; Jones, P. G.; Magull, J.; Ringe, A.; Oswald, R. B. *Inorg. Chem.* **2008**, *47*, 2171–2179. (d) Schaub, T.; Backes, M.; Radius, U. *Eur. J. Inorg. Chem.* **2008**, *17*, 2680–2690.

(26) Schaub, T.; Fischer, P.; Steffen, A.; Braun, T.; Radius, U.; Mix, A. *J. Am. Chem. Soc.* **2008**, *130*, 9304–9317.

(27) We see no H–F coupling on either the hydride or fluoride resonances. As any coupling would be <10 Hz, we assume it may be lost in the line width of the signals.

(28) Poulton, J. T.; Sigalas, M. P.; Folting, K.; Streib, W. E.; Eisenstein, O.; Caulton, K. G. *Inorg. Chem.* **1994**, *33*, 1476–1485.

(29) Poulton, J. T.; Sigalas, M. P.; Eisenstein, O.; Caulton, K. G. *Inorg. Chem.* **1993**, *32*, 5490–5501.

(30) There is no suggestion of any reaction between **5** and Me_3SiCF_3 to give a Ru– CF_3 complex. See: (a) Huang, D. J.; Koren, P. R.; Folting, K.; Davidson, E. R.; Caulton, K. G. *J. Am. Chem. Soc.* **2000**, *122*, 8916–8931.

(31) The inability to completely remove PPh_3 from samples of **6**, **7**, and **11** prevented us from attaining accurate elemental analysis on these compounds (see Experimental Section). To prove their integrity, they were trapped (along with **5**) by CO to give the corresponding dicarbonyl complexes $\text{Ru}(\text{NHC})(\text{PPh}_3)(\text{CO})_2\text{HF}$ (NHC = SIMes **17**, SIPr **18**, IPr **19**, IMes **20**), which were analytically and structurally characterized (CCDC 697992–697995). See Supporting Information for details.

(32) Efforts to use the phosphine sponge $\text{Pd}(\text{CH}_3\text{CN})_2\text{Cl}_2$ to isolate clean samples of **6** and **7** proved unsuccessful, as the addition of 1 equiv of the Pd complex turned yellow solutions of both Ru complexes brown (to black after 12 h at room temperature) and generated a mixture of four new hydride containing species.

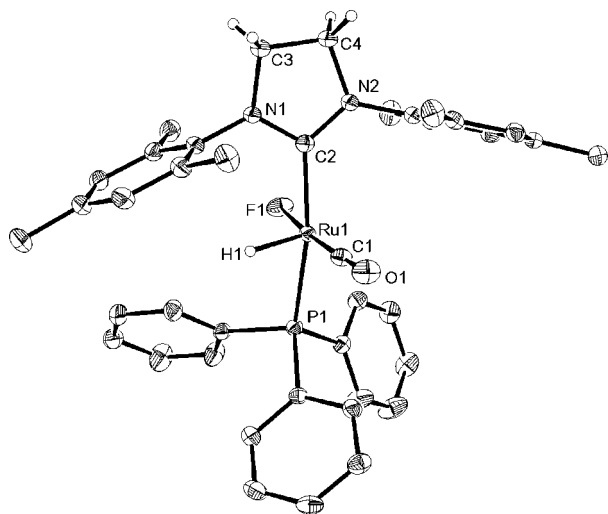


Figure 1. X-ray crystal structure of Ru(SIMes)(PPh₃)(CO)HF **5**. Thermal ellipsoids are shown at the 30% level. All hydrogen atoms (except the NHC backbone hydrogens and Ru–H) are omitted for clarity. Selected bond lengths (Å) and angles (deg): Ru(1)–C(1) 1.800(2), Ru(1)–C(2) 2.071(2), Ru(1)–F(1) 2.0172(13), Ru(1)–P(1) 2.3494(5), C(2)–Ru(1)–P(1) 168.44(6), F(1)–Ru(1)–C(1) 174.64(8), N(1)–C(2)–N(2) 108.25(18).

produced. A much cleaner synthetic pathway to **11** involved treatment of the dihydride complex Ru(IMes)(PPh₃)₂(CO)H₂ (**16**) with 1 equiv of Et₃N·3HF (Scheme 3).³³ The compound showed analogous solution behavior to **6** and **7** with low temperature coordination of PPh₃ to give Ru(IMes)(PPh₃)₂(CO)HF (**12**).³⁴

X-ray Crystal Structures of Ru(SIMes)(PPh₃)(CO)HF and Ru(IMes)(PPh₃)(CO)HF. The molecular structures of the five coordinate N-mesityl substituted products **5** and (more fortuitously) **11** are shown in Figures 1 and 2. As expected, both compounds display square pyramidal geometries at the ruthenium centers with the hydride ligand in the apical site trans to a vacant coordination site and fluoride *trans* to CO. While the OC–Ru–F angle in **5** is similar to that for the major disordered component in **11**, the C_{NHC}–Ru–PPh₃ angle is ca. 5° wider in **11**. Although no significant difference is seen in the two Ru–C_{NHC} bond lengths, the Ru–F distance in **5** is significantly shorter than that measured in **11** (2.0172(13) and 2.0315(13) Å, respectively).³⁵ On the basis that this implies greater π -donation in the former, the expected shorter Ru–CO and longer C–O distances are found.

Characterization of Ru(NHC)(PPh₃)₂(CO)H₂ and Reactions with C–F Bonds. Due to the difficulty noted earlier in completely separating complexes **6**, **7**, and **11** from PPh₃, reactivity studies of these compounds, along with **5**, were performed with samples in which free phosphine was present. Thus, at room temperature, **5–7** and **11** reacted with Et₃SiH within minutes to generate Et₃SiF and afford the bis-phosphine dihydride compounds

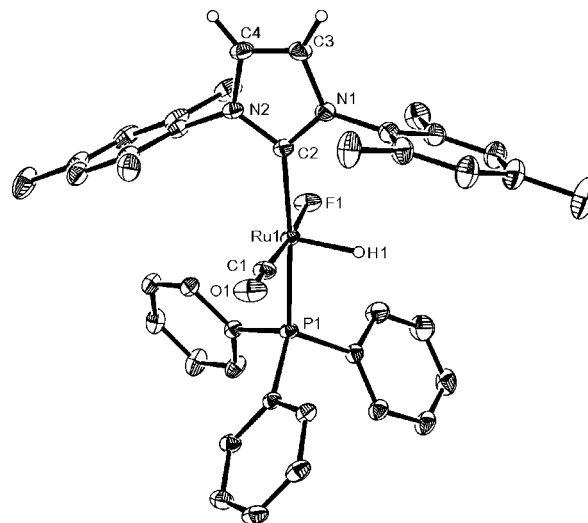
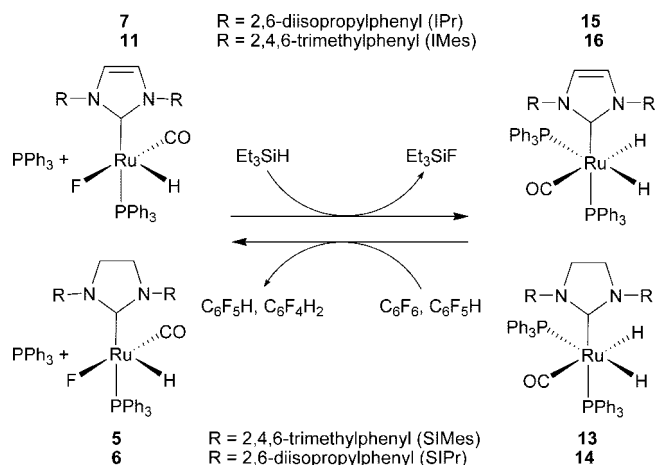


Figure 2. X-ray crystal structure of Ru(IMes)(PPh₃)(CO)HF **11**. Thermal ellipsoids are shown at the 30% level. All hydrogen atoms (except the NHC backbone hydrogens and Ru–H) and the solvent molecule are omitted for clarity. Selected bond lengths (Å) and angles (deg): Ru(1)–C(1) 1.820(3), Ru(1)–C(2) 2.077(2), Ru(1)–F(1) 2.0315(13), Ru(1)–P(1) 2.3403(6), C(2)–Ru(1)–P(1) 173.28(6), F(1)–Ru(1)–C(1) 174.13(16), N(1)–C(2)–N(2) 103.61(18).

Scheme 4



Ru(NHC)(PPh₃)₂(CO)H₂ (NHC = SIMes **13**, SIPr **14**, IPr **15**, IMes **16**). Compounds **13–15** (**16** was reported by us some time ago upon heating Ru(PPh₃)₃(CO)H₂ with IMes^{36,37}) were fully characterized by a combination of NMR and IR spectroscopies, elemental analysis, and X-ray crystallography. Each complex displayed two multiplet hydride resonances at δ –6.3 to δ –6.6 and δ –8.1 to δ –8.4, with coupling constants consistent with a geometry in which the hydrides are *trans* to CO and PPh₃ and the NHC ligands are *trans* to one of the phosphines (Scheme 4). It is worth noting that, in contrast to **16**, we had not previously been able to prepare **13–15** in even moderate yields upon heating Ru(PPh₃)₃(CO)H₂ with SIMes, SIPr, or IPr. It is unclear why these three carbenes behave differently to IMes in not fully substituting one of the phosphine ligands.

The X-ray crystal structures of **13–15** are shown in Figure 3, with pertinent bond angles and distances reported in Table

(33) Complexes **5–7** could also be formed the same way starting with complexes **13–15**.

(34) The solution IR spectra of **6**, **7**, and **11** all showed two carbonyl absorption bands at 1922/1907, 1919/1906, and 1913/1903 cm^{–1}, respectively, consistent with the presence of both Ru(NHC)(PPh₃)₂(CO)HF and Ru(NHC)(PPh₃)₂(CO)HF. Upon addition of excess phosphine to each of the solutions, the higher frequency bands disappeared leaving single carbonyl stretches at 1907, 1905, and 1902 cm^{–1}. See ref 28 for a comparison of other 16- and 18e ruthenium monocarbonyl complexes.

(35) X-ray and neutron structures of Ru(IMes)₂(CO)HF yielded Ru–F distances of 2.0326(15) and 2.042(6) Å, respectively. See ref 25b.

(36) Jazzar, R. F. R.; Macgregor, S. A.; Mahon, M. F.; Richards, S. P.; Whittlesey, M. K. *J. Am. Chem. Soc.* **2002**, *124*, 4944–4945.

(37) Jazzar, R. F. R. PhD Thesis, University of Bath, 2003.

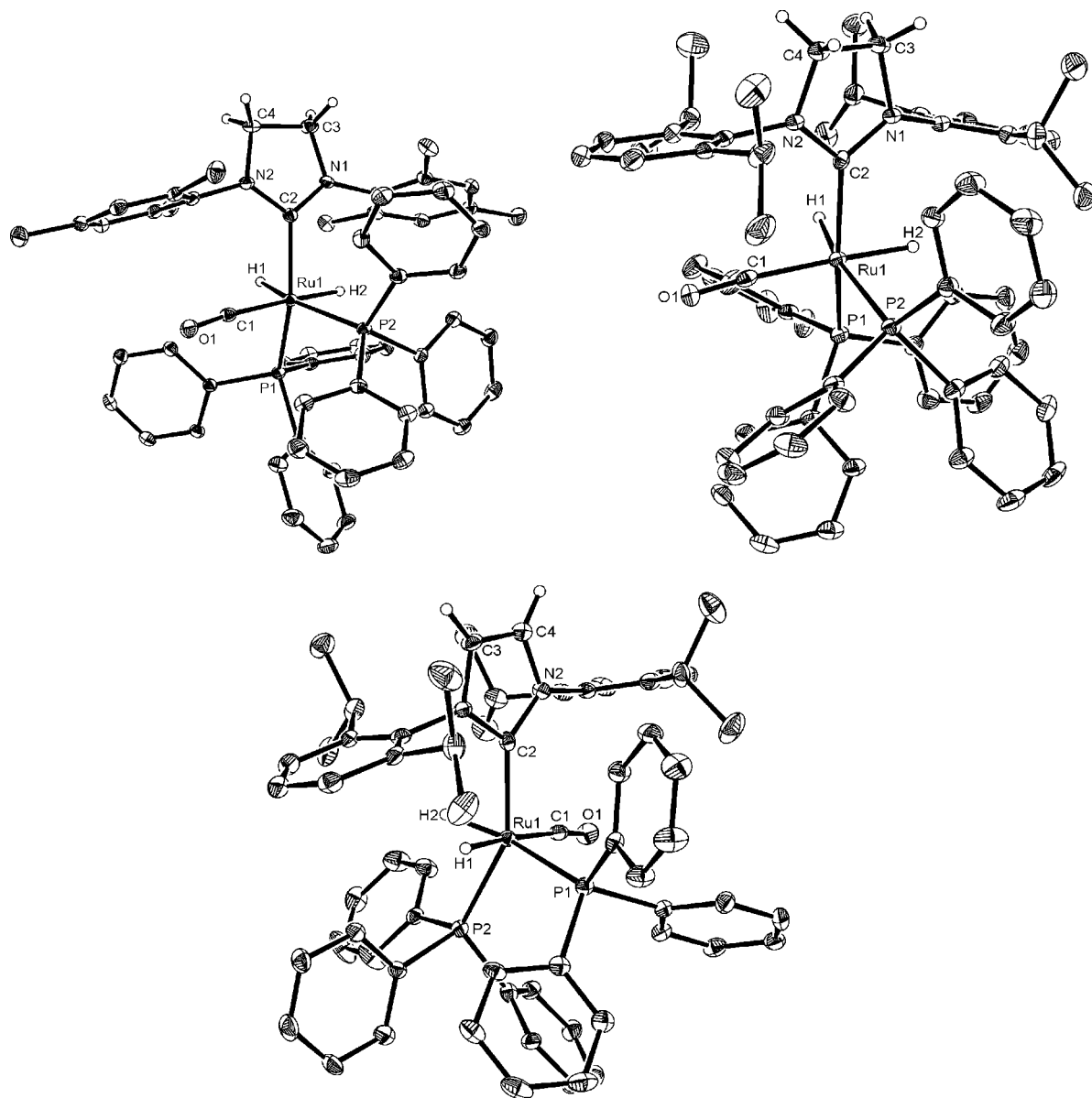


Figure 3. X-ray crystal structures of Ru(SIMes)(PPh₃)₂(CO)H₂ **13**, Ru(SIPr)(PPh₃)₂(CO)H₂ **14**, and Ru(IPr)(PPh₃)₂(CO)H₂ **15**. Thermal ellipsoids are shown at the 30% level. All hydrogen atoms (except the NHC backbone hydrogens and Ru–H) are omitted for clarity, as are the solvent molecules present in **14** and **15**.

Table 1. Selected Bond Lengths (Å) and Angles (deg) for Ru(NHC)(PPh₃)₂(CO)H₂ (NHC = SIMes **13**, SIPr **14**, IPr **15**, IMes **16**)

	13	14	15	16^a
Ru–NHC	2.097(3)	2.085(3)	2.087(4)	2.0956(17)
Ru–CO	1.910(3)	1.889(4)	1.897(5)	1.9145(17)
Ru–P _{trans} to NHC	2.3058(8)	2.3473(9)	2.3333(12)	2.2985(5)
Ru–P _{trans} to H	2.3622(10)	2.3850(9)	2.3832(11)	2.3628(4)
<i>trans</i> -NHC–Ru–P	145.49(9)	151.97(9)	152.83(11)	146.33(5)
<i>cis</i> -NHC–Ru–P	106.30(10)	104.69(9)	104.11(11)	104.94(5)
OC–Ru–P _{trans} to NHC	97.71(10)	93.27(11)	92.13(14)	94.76(5)
OC–Ru–P _{cis} to NHC	100.36(11)	97.63(11)	98.65(14)	100.65(5)
N–C–N	105.3(3)	102.1(3)	101.5(3)	101.55(14)

^a Data taken from ref 37.

1. In line with the structures of **16**³⁷ and other Ru(NHC)(PPh₃)₂(CO)H₂ compounds,^{38,39} all three compounds show distorted octahedral geometries with *trans*-C_{NHC}–Ru–P angles of 145.49(9)° (**13**), 151.97(9)° (**14**), and 152.83(11)° (**15**) (cf. 146.33(5)° in **16**).³⁷ As in **5** and **11**, and in a number of

other cases now reported, the M–NHC bond lengths are the same for both unsaturated and saturated carbene ligands.⁴⁰

When complexes **13–15** were heated at 343 K for 15 h in the presence of 10 equiv of C₆F₆ in THF-*d*₈, C–F bond

- (38) (a) Burling, S.; Mahon, M. F.; Paine, B. M.; Whittlesey, M. K.; Williams, J. M. J. *Organometallics* **2004**, *23*, 4537–4539. (b) Burling, S.; Kociok-Köhn, G.; Mahon, M. F.; Whittlesey, M. K.; Williams, J. M. J. *Organometallics* **2005**, *24*, 5868–5878.
- (39) Burling, S.; Paine, B. M.; Nama, D.; Brown, V. S.; Mahon, M. F.; Prior, T. J.; Pregosin, P. S.; Whittlesey, M. K.; Williams, J. M. J. *J. Am. Chem. Soc.* **2007**, *129*, 1987–1995.
- (40) (a) Hillier, A. C.; Sommer, W. J.; Yong, B. S.; Petersen, J. L.; Cavallo, L.; Nolan, S. P. *Organometallics* **2003**, *22*, 4322–4326. (b) Viciu, M. S.; Navarro, O.; Germaine, R. F.; Kelly, R. A.; Sommer, W. J.; Marion, N.; Stevens, E. D.; Cavallo, L.; Nolan, S. P. *Organometallics* **2004**, *23*, 1629–1635. (c) Kelly, R. A.; Scott, N. M.; Díez-González, S.; Stevens, E. D.; Nolan, S. P. *Organometallics* **2005**, *24*, 3442–3447. (d) Dorta, R.; Stevens, E. D.; Scott, N. M.; Costabile, C.; Cavallo, L.; Hoff, C. D.; Nolan, S. P. *J. Am. Chem. Soc.* **2005**, *127*, 2485–2495. (e) de Frémont, P.; Scott, N. M.; Stevens, E. D.; Nolan, S. P. *Organometallics* **2005**, *24*, 2411–2418.

Table 2. Catalytic Hydrodefluorination (HDF) of C₆F₆ (Entries 1–4) and C₆F₅H (Entries 5–8) with Et₃SiH by Ru(NHC)(PPh₃)₂(CO)H₂ (NHC = SIMes **13**, SIPr **14**, IPr **15**, IMes **16**)^a

entry	catalyst	product distribution (%)	selectivity ^b (%)	TON ^c	TOF ^d (h ⁻¹)
1	13	C ₆ F ₅ H (44.9), 1,2-C ₆ F ₄ H ₂ (7.6), 1,4-C ₆ F ₄ H ₂ (0.5)	–	6.1	0.31
2	14	C ₆ F ₅ H (14.2), 1,2-C ₆ F ₄ H ₂ (1.6), 1,4-C ₆ F ₄ H ₂ (0.1)	–	1.8	0.09
3	15	C ₆ F ₅ H (32.2), 1,2-C ₆ F ₄ H ₂ (19.9), 1,4-C ₆ F ₄ H ₂ (0.9)	–	7.4	0.37
4	16	C ₆ F ₅ H (18.0), 1,2-C ₆ F ₄ H ₂ (10.3), 1,4-C ₆ F ₄ H ₂ (0.3)	–	3.9	0.20
5	13	1,2-C ₆ F ₄ H ₂ (61.2), 1,4-C ₆ F ₄ H ₂ (1.1)	98.2	6.3	0.32
6	14	1,2-C ₆ F ₄ H ₂ (24.8), 1,4-C ₆ F ₄ H ₂ (1.0)	96.2	2.7	0.14
7	15	1,2-C ₆ F ₄ H ₂ (67.7), 1,4-C ₆ F ₄ H ₂ (1.6)	97.7	7.0	0.36
8	16	1,2-C ₆ F ₄ H ₂ (10.9), 1,4-C ₆ F ₄ H ₂ (0.9)	92.2	1.3	0.07

^a Reaction conditions: 0.01 M Ru(NHC)(PPh₃)₂(CO)H₂, THF solution, 0.1 M fluoroarene, 0.2 M Et₃SiH, 343 K for 19.45 h. ^b Selectivity is given as the % of main HDF product/total % of HDF products. ^c TON = (moles of fluoroaromatic product(s) multiplied by the no. of HDF steps)/moles of catalyst. ^d TOF = TON/h.

activation of the fluoroarene took place to give the hydride fluoride complexes **5**–**7** (Scheme 4) and 1 equiv of the HDF product C₆F₅H (characterized by the appearance of ¹H and ¹⁹F NMR resonances at δ 6.8, and δ –142, –158, and –166).⁴¹ While C–F cleavage also proceeded when **16** was heated with C₆F₆, the ruthenium containing products consisted of the corresponding hydride fluoride complex **11** in a 3:2 ratio with the carbene loss product Ru(PPh₃)₃(CO)HF. Further studies with the IPr complex **15** showed that C–F activation also occurred with C₆F₅H, resulting again in the formation of **7** and now 1,2-C₆F₄H₂ (vide infra). In contrast to previous reports involving the reactions of Ru–H complexes with C–F bonds, there was no evidence by NMR for the formation of any ruthenium fluoroaryl hydride products.^{24,42}

Catalytic Hydrodefluorination of C₆F₆ and C₆F₅H. In light of the interconversion of complexes **5**–**7** and **11** with **13**–**16** by reaction with Et₃SiH and C₆F₆ or C₆F₅H, catalytic HDF of aromatic fluorocarbons was attempted. The activity of the dihydride complexes **13**–**16** was screened at 10 mol% catalyst loading with C₆F₆ in the presence of 2 equiv of Et₃SiH in THF at 343 K for ca. 20 h.⁴³ The results are summarized in Table 2. All four complexes catalyzed HDF of C₆F₆ to give a mixture of C₆F₅H and C₆F₄H₂ (entries 1–4). The IPr complex **15** proved to be the most effective catalyst, giving 7.4 turnovers, followed by **13** (SIMes) > **16** (IMes) > **14** (SIPr).⁴⁴ NMR spectra recorded at the end of the catalytic reactions revealed, however, that only **15** remained intact, with the other three precatalysts having eliminated their carbene ligands over the course of the 20 h reaction time to leave Ru(PPh₃)₃(CO)H₂ as the major identifiable metal containing species. This complex was found

to be catalytically inactive showing that the NHC ligands play a key role in the behavior of these ruthenium systems. A series of kinetic experiments were performed (with only 1 equiv of silane added and at a slightly lower temperature of 339 K) in which the initial rates of formation of C₆F₄H₂ were monitored by ¹⁹F NMR for the different ruthenium precursors (Figure 4).^{45,46} Linear behavior was observed with the kinetic activity also in the order **15** > **13** > **16** > **14**.

For all of the ruthenium catalysts, HDF of C₆F₆ gave C₆F₅H as the major product. Of most interest, however, was the fact that the C₆F₄H₂ that was formed was mostly the 1,2-isomer rather than the 1,4-isomer (this was established by comparison to ¹⁹F NMR spectra of authentic samples of both compounds). This was investigated further using C₆F₅H as the starting fluoroarene, and selectivities of 92–98% for 1,2-C₆F₄H₂ were found,¹³ with turnover numbers about the same as those with C₆F₆. Consideration of the data in Table 2 shows that, in terms of activity, both **13** and **15** prove to be more efficient HDF catalysts toward C₆F₆ and C₆F₅H than Holland's iron diketiminate based system, which gave a maximum TON of 2.5 (TOF = 0.026 h⁻¹ at 318 K) with Et₃SiH as the reductant.²² The combination of Rh(PMe₃)₃(C₆F₅) and (EtO)₃SiH was reported to give TONs of 30–40 (TOF = 0.68–0.79 h⁻¹ at 367 K) for both substrates.²⁰ Prompted by the good activity and high stability of **15** noted above, HDF of C₆F₅H with Et₃SiH was performed at a lower catalyst loading (0.21 mol%, no solvent) in a catalytic run lasting 400 h and resulted in a turnover number of 202, corresponding to a turnover frequency (TOF) of 0.51 h⁻¹.⁴⁷ The TOF was raised to 0.86 h⁻¹ upon increasing the temperature to 363 K (TON of 62.2 after 72 h of reaction), although a further temperature rise to 393 K had an adverse effect on the rate of reaction (TOF = 0.16 h⁻¹ with TON of 11.6 after 72 h), presumably due to catalyst instability.

Further studies on the HDF of C₆F₅H by **15** revealed a drop in activity by a factor of 2 upon changing the solvent from THF to C₆H₆ (Table 3, entries 1 and 3). While this may simply reflect the influence of solvent polarity on the catalysis,²² an additional contributing factor may be a side reaction involving C–H activation which was observed when deuterated aromatic solvents were used.⁴⁸ Thus, reactions of both C₆F₆ and C₆F₅H in either C₆D₆ or C₆D₅CD₃ gave both C₆F₅D and C₆F₄D₂ along with C₆F₅H and 1,2-C₆F₄H₂. The deuterated compounds made up 6–15% of the total product distribution and were identified by the appearance of their ¹⁹F resonances at slightly lower frequency than the protio isotopomers. None of the deuterated products were observed in THF-d₈.⁴⁹

(45) Espenson, J. H. *Chemical Kinetics and Reaction Mechanisms*, 2nd ed; McGraw-Hill: New York, 1995.

(46) Kinetic experiments were run in THF at 339 K, the boiling point of the solvent.

(47) Turnover numbers of up to 90 have been recorded by Braun and co-workers for the conversion of hexafluoropropene into 3,3-trifluoropropylsilanes. See ref 17j.

(48) We and others have shown previously that Ru–NHC complexes can bring about bond activation of aromatic solvents. Thus, in ref 36 we reported that thermolysis of **16** in C₆D₆ led to a mixture of products including **16**-HD, Ru(IMes)₂(PPh₃)(CO)H₂, Ru(IMes)₂(PPh₃)(CO)HD, Ru(PPh₃)₃(CO)H₂, and Ru(PPh₃)₃(CO)HD. Leitner and co-workers subsequently showed that the dihydrogen dihydride complex Ru(IMes)(P-Cy₃)(η²-H₂)₂ was able to induce H/D exchange of C₆D₅CD₃ at room temperature. The resulting organometallic complex, which was now labeled Ru–D, Ru(η²-D₂) and at the ortho-mesityl groups, was subsequently used to introduce deuterium into a range of aromatic substrates including benzene, aniline, and anisole. Giunta, D.; Hölscher, M.; Lehmann, C. W.; Mynott, R.; Wirtz, C.; Leitner, W. *Adv. Synth. Catal.* **2003**, *345*, 1139–1145.

(41) The reaction was slowed considerably in the presence of 3 equiv of PPh₃ or upon changing the solvent to pyridine-d₅.

(42) Jasim, N. A.; Perutz, R. N.; Foxon, S. P.; Walton, P. H. *J. Chem. Soc., Dalton Trans.* **2001**, 1676–1685.

(43) The rapid room temperature reactions of **5**–**7** and **11** with alkylsilanes prevented us from using the Ru(NHC)(PPh₃)(CO)HF complexes as catalytic precursors as they were simply transformed into complexes **13**–**16** under the reaction conditions.

(44) TON is defined as (the number of moles of fluoroaromatic product(s) multiplied by no. of HDF steps)/number of moles of catalyst.

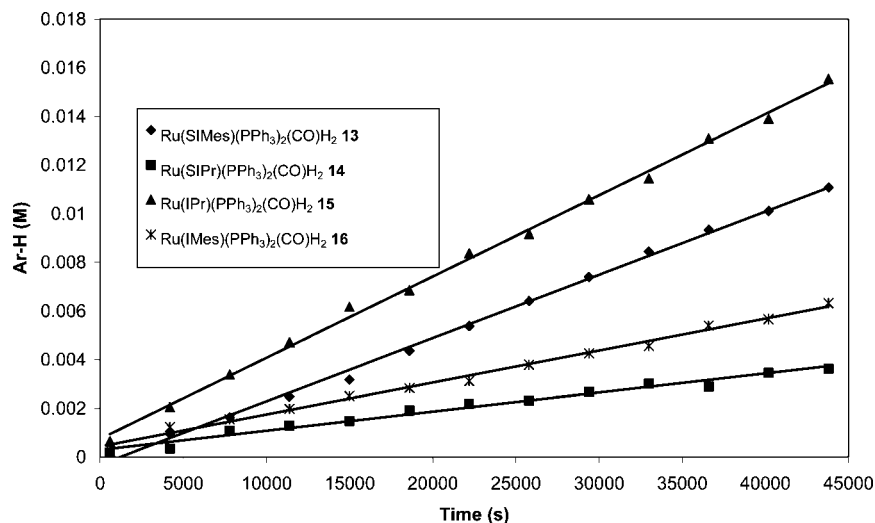


Figure 4. Time course plot of the catalytic HDF of C_6F_5H (THF, 339 K) by $Ru(NHC)(PPh_3)_2(CO)H_2$ (NHC = SIMes **13**, SIPr **14**, IPr **15**, and IMes **16**) showing changes in the rates upon variation of the Ru–NHC precursor ($[Et_3SiH] = [C_6F_5H] = 0.1$ M, $[Ru] = 0.01$ M).

Table 3. Catalytic Hydrodefluorination (HDF) of Fluoroarenes by $Ru(IPr)(PPh_3)_2(CO)H_2$ (**15**)^a

entry	substrate	solvent	silane	product distribution (%)	selectivity ^b (%)	TON ^c	TOF ^f (h ⁻¹)
1	C_6F_5H	THF	Et_3SiH	1,2- $C_6F_4H_2$ (67.7), 1,2- $C_6F_4H_2$ (1.6)	97.7	7.0	0.36
2 ^d	C_6F_5H	THF	Et_3SiH	1,2- $C_6F_4H_2$ (86.0), 1,2- $C_6F_4H_2$ (1.8)	97.9	8.9	0.19
3	C_6F_5H	benzene	Et_3SiH	1,2- $C_6F_4H_2$ (31.7), 1,4- $C_6F_4H_2$ (0.5)	98.4	3.3	0.17
4 ^e	C_6F_5H	toluene	Et_3SiH	1,2- $C_6F_4H_2$ (62.6), 1,4- $C_6F_4H_2$ (2.4)	96.3	6.5	0.33
5	C_6F_5H	THF	iPr_3SiH	1,2- $C_6F_4H_2$ (60.7), 1,4- $C_6F_4H_2$ (1.2)	98.1	6.2	0.32
6	C_6F_5H	THF	Ph_2MeSiH	1,2- $C_6F_4H_2$ (35.8), 1,4- $C_6F_4H_2$ (6.5)	84.6	4.3	0.22
7	C_6F_5H	THF	Ph_3SiH	1,2- $C_6F_4H_2$ (45.8), 1,4- $C_6F_4H_2$ (2.4)	95.0	4.9	0.25
8	C_6F_5H	THF	$(EtO)_3SiH$	1,2- $C_6F_4H_2$ (2.5), 1,4- $C_6F_4H_2$ (0.3)	88.7	0.3	0.02
9	C_6F_5H	THF	$Et_3SiH/1$ atm H_2	1,2- $C_6F_4H_2$ (66.4), 1,4- $C_6F_4H_2$ (1.2)	98.2	6.8	0.35
10	C_6F_5H	THF	$Et_3SiH/1$ atm O_2	1,2- $C_6F_4H_2$ (5.0), 1,4- $C_6F_4H_2$ (1.3)	79.1	0.7	0.04
11	C_6F_5H	THF	$Et_3SiH/0.03$ M PPh_3	1,2- $C_6F_4H_2$ (2.9), 1,4- $C_6F_4H_2$ (0.4)	87.8	0.4	0.02
12	C_6F_5H	THF	$Et_3SiH/0.03$ M Et_3N	1,2- $C_6F_4H_2$ (57.5), 1,4- $C_6F_4H_2$ (1.6)	97.3	6.0	0.31
13	C_6F_5H	THF	$Et_3SiH/0.03$ M DHA	1,2- $C_6F_4H_2$ (56.3), 1,4- $C_6F_4H_2$ (1.7)	97.0	5.8	0.30
14	C_6F_5H	THF	$Et_3SiH/0.03$ M C_8F	1,2- $C_6F_4H_2$ (54.7), 1,4- $C_6F_4H_2$ (1.3)	97.6	5.6	0.29
15	$C_6F_5CF_3$	THF	Et_3SiH	2,3,4,5- $C_6F_4HCF_3$ (3.1), 2,3,5,6- $C_6F_4HCF_3$ (14.1), 2,3,6- $C_6F_3H_2CF_3$ (3.3)	–	2.6	–
16	C_3F_5N	THF	Et_3SiH	2,3,4,5- C_3F_4HN (23.8), 2,3,5,6- C_3F_4HN (15.9), 2,3,5- $C_3F_3H_2N$ (8.2), 3,4,5- $C_3F_3H_2N$ (35.1), 3,4- $C_3F_2H_3N$ (3.2)	–	13.6	–

^a Reaction conditions: 0.01 M **15**, 0.1 M fluoroarene, 0.2 M silane, 343 K for 19.45 h unless otherwise stated. ^b Selectivity is given as the % of main HDF product/total % of HDF products. ^c TON = (moles of fluoroaromatic product(s) multiplied by the no. of HDF steps)/moles of catalyst. ^d Reaction run at 343 K for 48 h. ^e Reaction run at 393 K for 19.45 h. ^f TOF = TON/h.

Table 3 shows that triethylsilane proved to be the most effective reductant as increasing the bulk of the R substituent on the silane led to a decrease in both the activity and selectivity of C_6F_5H hydrodefluorination (Table 3, entries 5 and 7: iPr_3SiH : TON = 6.2, selectivity 98.1%; Ph_3SiH : TON = 4.9, selectivity 95.0%). Similarly, changes to the electronic structure at silicon reduced activity even further (entry

6: Ph_2MeSiH : TON = 4.3, selectivity 84.6%) or shut it down altogether (entry 8: $(EtO)_3SiH$: TON = 0.3).

Catalytic HDF of Other Perfluoroarenes. Attempts to conduct hydrodefluorination on other fluoroaromatic substrates met with mixed success (Table 3, entries 15–16). After 20 h of reaction, $C_6F_5CF_3$ gave a mixture of three products, 2,3,5,6- $C_6F_4HCF_3$

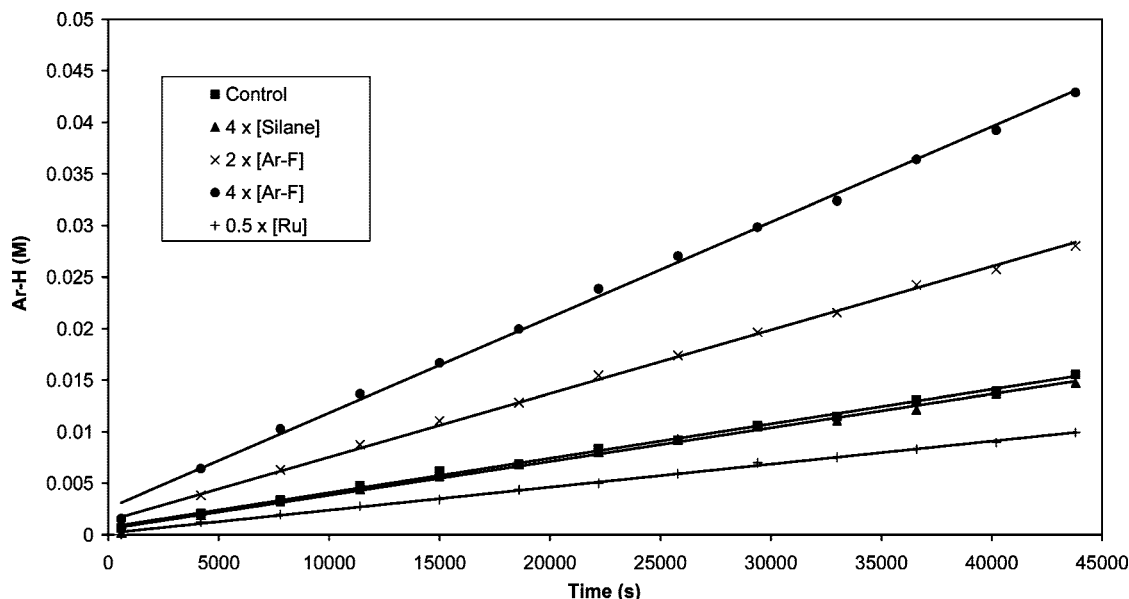


Figure 5. Time course plot of the catalytic HDF of C_6F_5H by $Ru(IPr)(PPh_3)_2(CO)H_2$ **15** (THF, 339 K) showing changes in the initial rates upon varying the concentrations of C_6F_5H , Et_3SiH and **15** versus a standard experiment ($[Et_3SiH] = [C_6F_5H] = 0.1$ M, $[15] = 0.01$ M).

(14.1%), 2,3,4,5- $C_6F_4HCF_3$ (3.1%), and 2,3,6- $C_6F_3H_2CF_3$ (3.3%).⁵⁰ Fluorocarbons with a lower fluorine content ($C_6F_5CH_3$, 2,3,4,5,6-pentafluorobiphenyl and both 1,2- and 1,4- $C_6F_4H_2$) were unreactive. Pentafluoropyridine proved to be highly active (TON = 13.6) although the hydrodefluorination was also the most unselective, with products resulting from one, two, and three HDF steps formed. The regioselectivity of the monodefluorination reaction followed that of C_6F_6 and C_6F_5H in giving substitution mostly at the 2-position, with more 2,3,4,5- C_5F_4HN (23.8%) formed than 2,3,5,6- C_5F_4HN (15.9%). Unlike C_6F_5H , however, further HDF of 2,3,4,5- C_5F_4HN occurred at both the 2- and 4-positions to give 3,4,5- $C_5F_3H_2N$ (35.1%) and 2,3,5- $C_5F_3H_2N$ (8.2%). Over a longer time, 3,4,5- $C_5F_3H_2N$ reacted further to afford small amounts of 3,4- $C_5F_2H_3N$.⁵¹

Mechanistic Studies of Catalytic HDF. A kinetic study of the HDF of C_6F_5H in the presence of Et_3SiH with **15** is summarized by the time course plots shown in Figure 5. In a series of experiments in which the formation of 1,2- $C_6F_4H_2$ was monitored by ^{19}F NMR in the presence of α,α,α -trifluorotoluene as a standard, the initial concentrations of C_6F_5H , Et_3SiH and **15** were varied while the other two were kept constant and the initial rates measured.⁴⁶ The plots indicate a first-order dependence with respect to the concentrations of both fluoroarene

Table 4. Initial Rates for the Catalytic Hydrodefluorination of C_6F_5H with Et_3SiH Using $Ru(IPr)(PPh_3)_2(CO)H_2$ (**15**) (THF- d_8 , 339 K)

entry	$[C_6F_5H]_0$ (M)	$[Et_3SiH]_0$ (M)	$[15]_0$ (M)	initial rate ($10^{-7} M^{-1} s^{-1}$)
1	0.1	0.1	0.01	3.34 ± 0.11
2	0.2	0.1	0.01	6.16 ± 0.17
3	0.4	0.1	0.01	9.25 ± 0.29
4	0.1	0.4 ^a	0.01	3.27 ± 0.13
5	0.1	0.1	0.005 ^b	2.23 ± 0.66
6 ^c	0.1	0.1	0.01	3.95 ± 0.12
7 ^c	0.1	0.1	0.01 + 0.0015 M PPh_3	3.53 ± 0.15
8 ^c	0.1	0.1	0.01 + 0.003 M PPh_3	1.94 ± 0.08
9 ^c	0.1	0.1	0.01 + 0.006 M PPh_3	1.35 ± 0.05

^a At $[Et_3SiH] = 0.02$ M, an initial rate of $(3.44 \pm 0.13) \times 10^{-7} M^{-1} s^{-1}$ was found. ^b A kinetic run with $[15] = 0.2$ M proved unreliable for kinetic analysis due to the incomplete solubility of the complex at this concentration. ^c Experiments run at 342 K.

and ruthenium precursor and a zero-order dependence on the concentration of silane (Table 4). These results suggest that the rate-limiting step in the catalytic cycle involves activation of the fluoroarene, in contrast to Holland's results on the β -diketiminate iron(II) system which showed that reaction with silane was rate-determining. It is worth reiterating an earlier point that whereas our Ru system will directly activate a C–F bond, the iron complex only performed C–F activation when silane was present.

HDF of C_6F_5H was shut down when either 1 atm of O_2 or 3 equiv of PPh_3 (see below) were added (Table 3, entries 10 and 11). Compared to a standard reference experiment (Table 3, entry 1), we found that the addition of Et_3N or CsF (3 equiv in each case) somewhat reduced the efficiency of the catalysis

(51) Similarly, analysis of the 1H NMR spectrum at the end of the catalytic reaction with pentafluoropyridine showed a broad doublet hydride signal at $\delta = 25.62$ ($^2J_{HP} = 23.50$ Hz), which showed an HMQC correlation to a broad ^{31}P resonance at $\delta 47.0$. We assign these signals as arising from $Ru(IPr)(PPh_3)(CO)(C_5F_4N)H$ on the grounds that the ^{19}F NMR showed four signals in a 1:1:1:1 ratio, which was correlated by ^{19}F – ^{19}F COSY. The appearance of a singlet at $\delta 4.3$ in the proton spectrum for H_2 is consistent with formation of the 2,3,5,6-tetrafluoropyridyl ligand by C–H activation of 2,3,5,6-tetrafluoropyridine.

(49) This contrasts with an earlier report (ref 16) employing $(\eta^5-C_5H_5)_2ZrCl_2/Mg/HgCl_2$ in which deuterium could be extracted from THF- d_8 .

(50) Analysis of the 1H NMR spectrum at longer times (ca. 85 h) showed the presence of a new ruthenium species assigned as the fluoroaryl hydride complex $Ru(IPr)(PPh_3)(CO)(C_6F_4CF_3)H$. This displayed a hydride resonance at $\delta = 25.83$ ($J_{HP} = 24.01$, $J_{HF} = 5.95$ Hz) with a doublet of triplets multiplicity and a singlet ^{31}P signal at $\delta 55.0$. The presence of a 2,3,5,6- $C_6F_4CF_3$ ligand was inferred from a ^{19}F – 1H HMBC experiment which showed a correlation from the hydride signal to two ^{19}F signals at $\delta = 111.1$ (dd, $J = 34.10$, $J = 15.62$ Hz) and $\delta = 117.6$ (multiplet). ^{19}F – ^{19}F COSY confirmed the presence of a further three ^{19}F resonances, two multiplets at $\delta = 146.3$ and $\delta = 148.6$, and a triplet at $\delta = 57.6$ ($J_{FF} = 21.68$ Hz). The proton spectrum also displayed the presence of free H_2 in solution, suggesting that coordination of the benzotrifluoride ligand occurs via activation of the C–H bond. This was confirmed by reaction of **15** with 5 equiv of 2,3,5,6- $C_6F_4HCF_3$ which generated a small amount of $Ru(IPr)(PPh_3)(CO)(C_6F_4CF_3)H$ at room temperature within 30 min of addition. Heating the solution to 343 K gave the product in a ratio of 1:1.5 with $Ru(IPr)(PPh_3)_2(CO)H_2$.

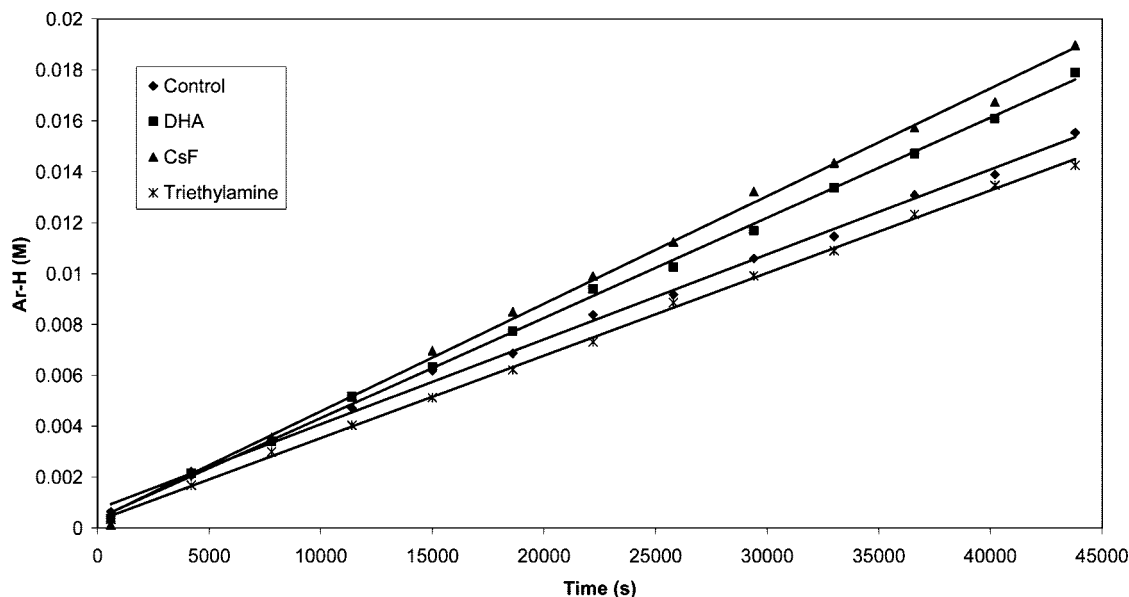


Figure 6. Time course plot of the catalytic HDF of C_6F_5H by $Ru(IPr)(PPh_3)_2(CO)H_2$ **15** (339 K, THF) showing changes in the initial rates upon addition of Et_3N , CsF , and dihydroanthracene (DHA) versus a standard experiment ($[Et_3SiH] = [C_6F_5H] = 0.1$ M, $[15] = 0.01$ M).

(Table 3, entries 12 and 14), although time course plots for each of these two additives showed no significant change to the kinetics (Figure 6).⁵² No change in TON or selectivity was observed when HDF of C_6F_5H with Et_3SiH was performed under 1 atm of H_2 rather than 1 atm of argon (Table 3, entry 9), showing that, at least at this pressure, dihydrogen is not a competent reductant. This was substantiated further by the complete removal of all silane and the attempted HDF of C_6F_5H with H_2 alone, which failed to give any $C_6F_4H_2$ even under 3 atm of H_2 .

The most commonly accepted pathways for C–F bond activation involve oxidative addition, nucleophilic substitution, or electron transfer.² Neither of the latter two mechanisms is consistent with the regioselectivity of the HDF products as both pathways would favor activation of a C–F bond *para* to an electron-withdrawing group; thus HDF of C_6F_5H should yield 1,4- $C_6F_4H_2$ rather than the 1,2-isomer which is observed. Similarly, as seen for a number of Rh⁵³ and Pd/Pt phosphine complexes,⁵⁴ nucleophilic substitution or electron transfer pathways would lead to activation of the *para*-C–F bond in pentafluoropyridine, whereas attack at the 2-position, as seen here and also for a number of Ni phosphine species,^{5,55} is more consistent with an oxidative addition process. Holland has also noted that, for electron transfer, catalytic conversion should correlate with the electron affinity of the perfluoroarene substrate, again something we do not observe.²² A common tool used for probing electron transfer involves addition of a radical trap, such as dihydroanthracene (DHA). In our case, we observe a negligible effect on the rate of HDF activity (Figure 6, Table 3).

Mechanistic cycles to explain both the inorganic and organic products formed under stoichiometric and catalytic conditions are proposed in Schemes 5 and 6 and involve oxidative addition/metathesis reactions of C–F and C–H bonds. A reaction pathway for fully fluorinated substrates (e.g., C_6F_6) is shown in Scheme 5. Facile dissociation of PPh_3 was supported by a series of kinetic experiments at variable $[PPh_3]$ (Table 4, entries 6–9) which revealed a close to inverse first-order dependence of catalytic activity on phosphine concentration. As these experiments were conducted with 0.15–0.6 equiv PPh_3 per Ru, this suggests that trapping of **I** (see Schemes 5 and 6) by PPh_3 to reform the 18e bisphosphine dihydride precursor must be very fast. Phosphine dissociation has also previously been reported by us for the analogous N-alkyl substituted complexes $Ru(NHC)(PPh_3)_2(CO)H_2$.³⁹ Under stoichiometric conditions (i.e., in the absence of R_3SiH), the resulting 16-electron five-coordinate species (**I**) could then “interact” with C_6F_6 (species **II**). As a formal oxidative addition reaction to Ru(II) seems unlikely,⁵⁶ we assume that coordination would involve one of the two accepted binding modes, either an $\eta^2-C_6F_6$ complex^{4,26,57} or a σ -aryl-F–M species.⁵⁸ In either case, subsequent metathesis⁵⁹ would lead to the formation of a new C–H bond, affording C_6F_5H and the final ruthenium containing species **7**.⁶⁰ Under catalytic conditions in which R_3SiH is present, **7**

(52) Thus, there is no evidence to suggest that fluoride promotes activation reactions, as seen by Edelbach and Jones (ref 6) with $(\eta^5-C_5Me_5)Rh(PMe_3)H_2$.

(53) Noveski, D.; Braun, T.; Neumann, B.; Stammler, A.; Stammler, H.-G. *Dalton Trans.* **2004**, 4106–4119.

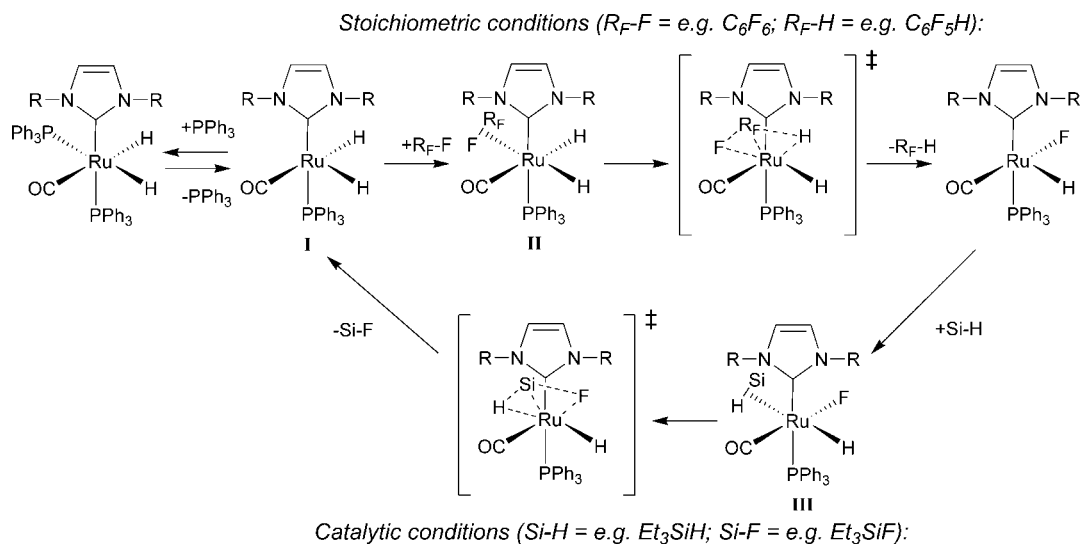
(54) Jasim, N. A.; Perutz, R. N.; Whitwood, A. C.; Braun, T.; Izundu, J.; Neumann, B.; Rothfeld, S.; Stammler, H.-G. *Organometallics* **2004**, *23*, 6140–6149.

(55) Archibald, S. J.; Braun, T.; Gaunt, J. A.; Hobson, J. E.; Perutz, R. N. *J. Chem. Soc., Dalton Trans.* **2000**, 2013–2018.

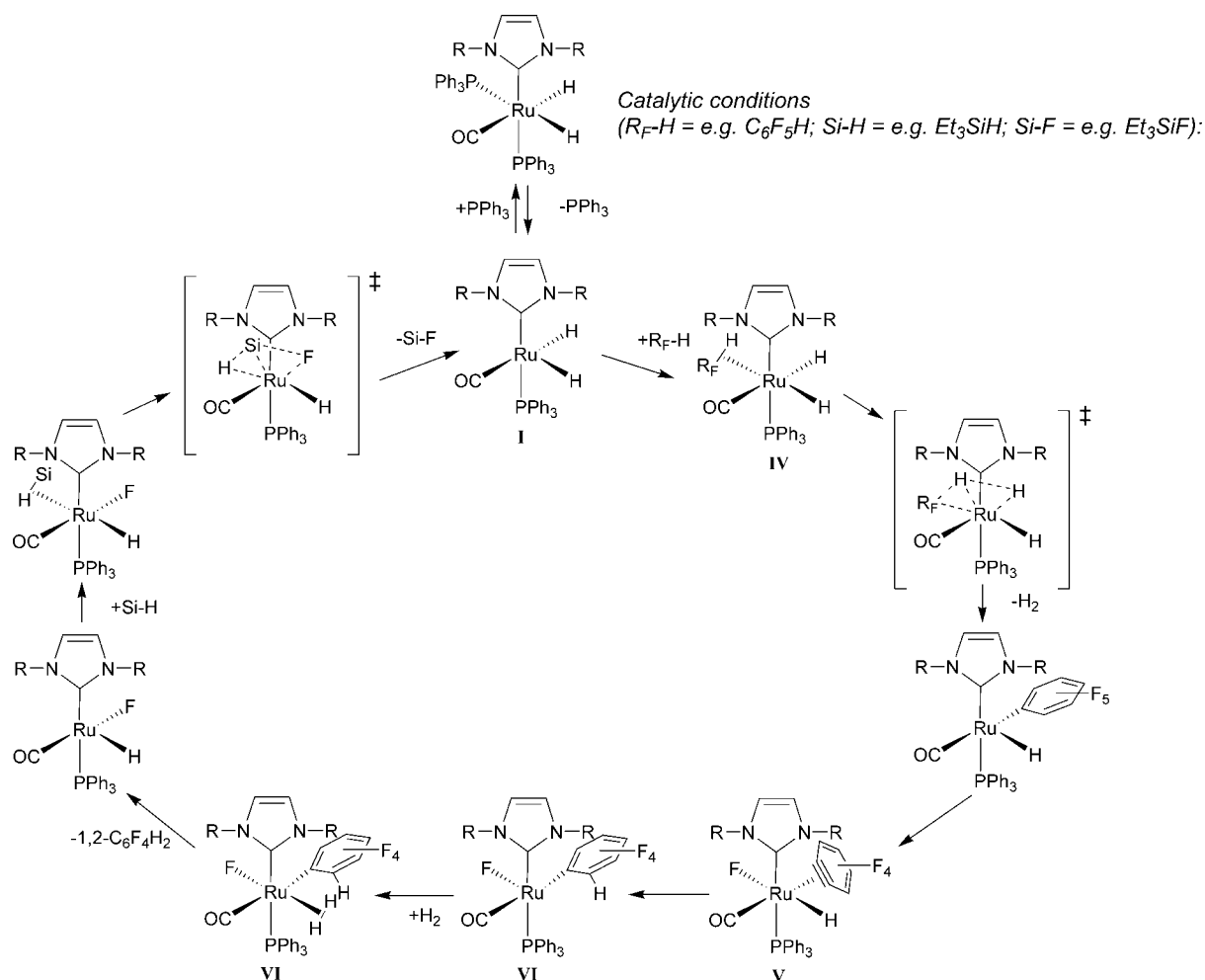
(56) While Ru(IV) di-, tri-, and indeed polyhydride complexes are known (e.g., $Ru(P^iPr_3)_2H_2Cl_2$ (Wolf, J.; Stüer, W.; Grünwald, C.; Gevert, O.; Laubender, M.; Werner, H. *Eur. J. Inorg. Chem.* **1998**, 1827–1834) and $(\eta^5-C_5Me_5)Ru(PR_3)_3$ (Rodriguez, V.; Donnadiu, B.; Sabo-Etienne, S.; Chaudret, B. *Organometallics* **1998**, *17*, 3809–3814), Kubas has noted that σ -coordination vs oxidation (e.g., $M(\eta^2-H_2)$ vs $H-M-H$) is highly ligand dependent and that CO ligands tend to favor σ -complexes. For this reason, we feel that σ -coordination of, for example, C_6F_6 to afford the Ru(II) species $Ru(NHC)(PPh_3)(CO)(\eta^2-C_6F_6)H_2$ is more likely than oxidative addition to give the ruthenium(IV) intermediate $Ru(NHC)(PPh_3)(CO)(C_6F_5)FH_2$. Kubas, G. J. *Metal Dihydrogen and σ -Bond Complexes*; Kuwer Academic: New York, 2001.

(57) (a) Belt, S. T.; Duckett, S. B.; Helliwell, M.; Perutz, R. N. *J. Chem. Soc., Chem. Commun.* **1989**, 928–929. (b) Braun, T.; Cronin, L.; Higgitt, C. L.; McGrady, J. E.; Perutz, R. N.; Reinhold, M. *New J. Chem.* **2001**, *25*, 19–21.

Scheme 5



Scheme 6



could form a σ -complex (**III**) with R_3SiH , which upon silyl group transfer would eliminate R_3SiF and reform **I**.⁶¹ Efforts to detect **III** proved unsuccessful, as addition of Et_3SiH to **7** at low temperature led to the formation of Et_3SiF even at 204 K.

The formation of 1,2- $C_6F_4H_2$ from C_6F_5H is consistent with a mechanism proposed in Scheme 6, in which **I** initially interacts

in such a way (e.g., an $\eta^2-C_6F_5H$ complex) to give **IV** in which the C–H bond (rather than C–F bond) is primed for reaction. Subsequent metathesis and elimination of H_2 would leave the fluoroaryl complex $Ru(IPr)(PPh_3)(CO)(C_6F_5)H$, which we then postulate could undergo a β -F transfer from the ring to the metal to give the tetrafluorobenzene hydride fluoride species **V**. Subsequent hydrogen transfer from Ru to the ring would yield

an *o*-C₆F₄H complex (VI). Reoordination of H₂ and metathesis would lead to the elimination of 1,2-C₆F₄H₂ and leave **7**, which then reacts with silane as in Scheme 5 to restart the catalytic cycle. At this time, we can only speculate on how the proposed catalytic cycle relates back to the kinetic experiments in, for example, explaining the first-order dependence on the concentration of fluoroarene. It also worth remembering that while varying the concentration of silane has no effect on the kinetics, both TON and selectivity were affected by different R groups on the silane, perhaps reflecting the ability of different silanes to form *σ*-silane complexes.

While problems of H/D exchange prevented us from measuring a kinetic isotope effect for the HDF reaction,⁶² a range of other experiments were performed in an effort to support the proposed mechanisms. Conclusive evidence for activation of the C–H rather than a C–F bond in partially fluorinated arenes was found upon reaction of Ru(IPr)(PPh₃)₂(CO)D₂ with C₆F₅H (10 equiv) at room temperature (THF-*d*₈) which generated C₆F₅D together with Ru(IPr)(PPh₃)₂(CO)HD and Ru(IPr)(PPh₃)₂(CO)H₂.⁶³ Many of the early studies on C–F bond activation also reported a preference for C–H over C–F activation in the reactions of C₆F₅H and other partially fluorinated substrates.^{4,64} More recently, calculations have been used to show that this preference is largely kinetic in origin.⁶⁵ For example, while for both of the coordinatively unsaturated fragments M(H₂PCH₂–CH₂PH₂) (M = Ni, Pt) C–F activation is the more thermodynamically favorable reaction, C–H activation (at least for Pt) is a more kinetically accessible process.⁷

- (58) (a) Bouwkamp, M. W.; De Wolf, J.; Del Heirro Morales, I.; Gercama, J.; Meetsma, A.; Troyanov, S. I.; Hessen, B.; Teuben, J. H. *J. Am. Chem. Soc.* **2002**, *124*, 12956–12957. (b) Bouwkamp, M. W.; Budzelaar, P. H. M.; Gercama, J.; Del Heirro Morales, I.; De Wolf, J.; Meetsma, A.; Troyanov, S. I.; Teuben, J. H.; Hessen, B. *J. Am. Chem. Soc.* **2005**, *127*, 14310–14319.
- (59) Perutz, R. N.; Sabo-Etienne, S. *Angew. Chem., Int. Ed.* **2007**, *46*, 2578–2592.
- (60) Deuterium labelling studies indicate that the mechanism is not altogether this simple since reaction of Ru(IPr)(PPh₃)₂(CO)D₂ with 10 equiv of C₆F₆ in THF-*d*₈ not only yields the expected C₆F₅D but also gives some C₆F₅H. The protio source appears to involve orthometallation of the PPh₃ ligands. See ref 62.
- (61) An alternative catalytic pathway could involve the initial reaction of **15** with R₃SiH rather than fluoroarene. Although no reaction was apparent when **15** was heated with 10 equiv of Et₃SiH at 343 K in C₆D₆, the formation of both Ru(IPr)(PPh₃)₂(CO)HD and Et₃SiH was seen at room temperature within 5 min of mixing when **15** was treated with Et₃SiD. Thus, reaction of **15** does occur with Si–H bonds at room temperature, although the formation of a RuH₂ rather than a Ru(SiR₃)H product implies that any initial reaction with silane would only serve to generate the catalytic intermediate **I**.
- (62) Measurement of a kinetic isotope effect using Ru(IPr)(PPh₃)₂(CO)D₂ was thwarted by D/H exchange. While the dideuteride can be prepared by simply placing Ru(IPr)(PPh₃)₂(CO)H₂ under 1 atm of D₂, we observed that efforts to maximize the level of D-incorporation by continually replenishing the D₂ atmosphere and leaving the reaction for longer led to broadening of the ³¹P NMR signals, suggestive of H/D exchange into the *ortho*-phenyl positions of the PPh₃ ligands. Thus a sample of Ru(IPr)(PPh₃)₂(CO)D₂ (ca. 78% RuD₂) was prepared from a single cycle of D₂ + Ru(IPr)(PPh₃)₂(CO)H₂, isolated, and then heated at 322 K for 1.5 h and followed by ¹H and ³¹P NMR; we observed clear H/D exchange into the *ortho*-phenyl protons leaving a mixture of the RuD₂, RuHD, and RuH₂ species. As this scrambling occurs some 20 K lower than the temperature used for catalysis (343 K), clearly RuD₂ would be exchanged before any KIE could be determined.
- (63) See refs 50 and 51.
- (64) Selmezy, A. D.; Jones, W. D.; Partridge, M. G.; Perutz, R. N. *Organometallics* **1994**, *13*, 522–532.

Efforts to support the intermediacy of a tetrafluorobenzene species proved less successful.⁶⁶ Jones and co-workers have shown that the decomposition of (η⁵-C₅H₅)₂Zr(C₆F₅)₂ gives (η⁵-C₅H₅)₂Zr(C₆F₅)F and tetrafluorobenzene (“C₆F₄”), which could be trapped as a Diels–Alder adduct with 2,3,5,6-tetramethylbenzene (durene).⁶⁷ However, later work showed that an intermediate Zr–C₆F₄ species proposed on the decomposition pathway of (η⁵-C₅Me₅)₂Zr(*o*-C₆FH₄)H to (η⁵-C₅Me₅)₂Zr(C₆H₅)F could not be trapped, possibly due to the tetrafluorobenzene remaining coordinated at all times to the Zr center.¹⁵ This may then also explain our lack of success in the trapping experiments with durene.⁶⁸

Conclusions

The N-aryl substituted N-heterocyclic carbene complexes Ru(NHC)(PPh₃)₂(CO)H₂ have been shown to be precursors for the catalytic hydrodefluorination (HDF) of aromatic fluorocarbons in the presence of alkyl silanes. Stoichiometric experiments have shown that the activity of these ruthenium dihydride species is based on their ability to abstract fluoride to give the coordinatively unsaturated species Ru(NHC)(PPh₃)₂(CO)HF, which undergo F/H exchange in the presence of a silane.

The most unusual aspect of the HDF chemistry is the high regioselectivity for formation of 1,2-partially fluorinated products starting from C₆F₅H. This substitution pattern contrasts with the 1,4-products reported by both Milstein and Holland for the Rh and Fe catalyzed reactions. Deuterium labeling experiments suggest that the selectivity in our Ru experiments arises out of a preference for C–H over C–F activation under catalytic conditions and may involve a fluorinated benzyne intermediate.

Together with the recent reports of C–F activation and C–C bond formation from the Radius group,¹⁸ our results suggest that interesting future developments on the functionalization of fluorocarbons may arise from metal–NHC complexes.

Experimental Section

General Comments. All manipulations were carried out under argon using standard Schlenk, high vacuum, or glovebox techniques under an atmosphere of argon. Solvents were purified using a MBraun SPS solvent system (hexane, Et₂O), Innovative Technologies solvent system (THF) or under a nitrogen atmosphere from sodium benzophenone ketyl (benzene, toluene) or Mg/I₂ (ethanol). NMR solvents (Fluorochem) were vacuum transferred from potassium (C₆D₆, C₆D₅CD₃, THF-*d*₈). Ru(PPh₃)₃(CO)H₂,⁶⁹ Ru(IMes)(PPh₃)₂(CO)H₂,³⁷ IMes,⁷⁰ IPr,⁷¹ SIMes(C₆F₅)H,⁷² and SIPr(C₆F₅)H⁷³ were prepared via literature methods. Fluorocarbons and silanes were dried over activated 3 Å molecular sieves and subsequently stored under argon.

¹H NMR spectra were recorded on Bruker Avance 400 and 500 MHz NMR spectrometers, at 298 K unless otherwise stated, and

- (65) Bosque, R.; Clot, E.; Fantacci, S.; Maseras, F.; Eisenstein, O.; Perutz, R. N.; Renkema, K. B.; Caulton, K. G. *J. Am. Chem. Soc.* **1998**, *120*, 12634–12640.
- (66) The first stable M(η²-C₆F₄) complexes were prepared relatively recently by Hughes and co-workers. (a) Hughes, R. P.; Williamson, A.; Sommer, R. D.; Rheingold, A. L. *J. Am. Chem. Soc.* **2001**, *123*, 7443–7444. (b) Hughes, R. P.; Laritchev, R. B.; Williamson, A.; Incarvito, C. D.; Zakharov, L. N.; Rheingold, A. L. *Organometallics* **2002**, *21*, 4873–4885.
- (67) (a) Edlbach, B. L.; Kraft, B. M.; Jones, W. D. *J. Am. Chem. Soc.* **1999**, *121*, 10327–10331. (b) Kraft, B. M.; Lachicotte, R. J.; Jones, W. D. *Organometallics* **2002**, *21*, 727–731.
- (68) Coordinated or trapped fluorobenzenes have also been described in the following cases: (a) Reference 9. (b) Keen, A. L.; Johnson, S. A. *J. Am. Chem. Soc.* **2006**, *128*, 1806–1807. (c) Werkema, E. L.; Andersen, R. A. *J. Am. Chem. Soc.* **2008**, *130*, 7153–7165.

referenced to benzene at δ 7.15 (^{13}C , δ 128.0), toluene at δ 2.04, or THF at δ 3.58. No effort was made to assign ^{13}C signals for the PPh_3 ligands unless specified. $^{31}\text{P}\{^1\text{H}\}$ NMR chemical shifts were referenced externally to 85% H_3PO_4 (δ 0.0), while ^{19}F spectra were referenced to CFCl_3 (δ 0.0). 2D experiments (^1H COSY, $^1\text{H}-\text{X}$ ($\text{X} = ^{13}\text{C}$, ^{31}P , ^{19}F) HMQC/HMBC) were performed using standard Bruker pulse sequences. IR spectra were recorded on a Nicolet Nexus FTIR spectrometer. Elemental analyses were conducted by Elemental Microanalysis Ltd., Okehampton, Devon, UK.

Ru(SIMes)(PPh₃)(CO)HF (5). Ru(PPh₃)₃(CO)HF (500 mg, 0.52 mmol) and SIMes(C₆F₅)H (760 mg, 1.60 mmol) were dissolved in benzene (20 mL) in an ampule fitted with a PTFE tap and heated at 343 K for 2.5 h. The resultant green solution was pumped to dryness, washed with hexane (50 mL), and dried in *vacuo* to yield Ru(SIMes)(PPh₃)(CO)HF. Yield (310 mg, 81%). A higher purity product could be obtained by treatment of a benzene solution (20 mL) of Ru(SIMes)(PPh₃)₂(CO)H₂ (**13**: 100 mg, 0.010 mmol) with Et₃N·3HF (18 mg, 0.011 mmol) and subsequent stirring at room temperature for 2 h. The resultant yellow solution was stirred with CsF (84 mg, 0.055 mmol) for 1 h, the solution filtered, and the filtrate reduced to dryness. The residue was washed with hexane (2 × 10 mL) to afford **5** as a yellow microcrystalline solid. Yield (60 mg, 75%). Crystals suitable for X-ray crystallography were obtained by layering a benzene solution with hexane. Analysis for C₄₃H₄₅N₂O₂PrRu·0.5C₆H₆ [found (calculated)]: C, 68.24 (68.21); H, 5.99 (6.11); N, 3.70 (3.64). ^1H NMR (C₆D₆, 400 MHz, 298 K): δ 7.40 (m, 6H, PC₆H₅), 6.97 (m, 9H, PC₆H₅), 6.85 (s, 2H, C₆Me₃H₂), 6.77 (s, 2H, C₆Me₃H₂), 3.28 (s, 4H, NCH₂), 2.65 (s, 6H, C-CH₃) 2.48 (s, 6H, C-CH₃), 2.10 (s, 6H, C-CH₃) -23.37 (d, $J_{\text{HP}} = 24.11$ Hz, 1H, Ru-H). $^{31}\text{P}\{^1\text{H}\}$: δ 38.8 (br d, $J_{\text{PF}} = 18.0$ Hz) [upon addition of Me₃SiCF₃, this becomes a sharper doublet with a resolved J_{FP} coupling of 26.7 Hz]. ^{19}F : δ 215.8 (br s), [upon addition of Me₃SiCF₃, this becomes a sharper doublet with a resolved J_{FP} coupling of 26.7 Hz]. $^{13}\text{C}\{^1\text{H}\}$: δ 217.0 (d, $J_{\text{CP}} = 99.3$ Hz, NCN), 205.4 (br s, Ru-CO), 138.5 (s, *o*-*p*-C₆Me₃H₂), 138.3 (s, *o*-*p*-C₆Me₃H₂), 137.0 (s, N-C_{ipso}), 136.3 (d, $J_{\text{CP}} = 39.0$ Hz, PC₆H₅), 135.3 (d, $J_{\text{CP}} = 12.1$ Hz, PC₆H₅), 130.3 (s, *m*-C₆Me₃H₂), 130.3 (s, *m*-C₆Me₃H₂), 129.9 (br s, PC₆H₅), 128.8 (s, PC₆H₅) 51.5 (s, NCH₂), 51.5 (s, N-CH₂), 21.8 (s, CCH₃), 19.3 (s, CCH₃), 19.2 (s, CCH₃). IR (C₆D₆, cm⁻¹): 1916 (ν_{CO}).

Ru(SIMes)(PPh₃)₂(CO)HF (8). Addition of 2.6 equiv of PPh₃ (5 mg, 0.018 mmol) to a solution of **5** (5 mg, 0.007 mmol) showed by low temperature NMR full conversion to **8**. Selected ^1H NMR (C₆D₅CD₃, 400 MHz, 201 K): δ 3.28–2.98 (br s, 3H, CH₃), 2.91 (br s, 3H, CH₃), 2.80 (br s, 3H, CH₃), 2.32 (br s, 6H, CH₃), 1.57 (br s, 3H, CH₃) -5.67 (dd, $J_{\text{HP}} = 118.02$, $J_{\text{HP}} = 28.00$ Hz, 1H, Ru-H). $^{31}\text{P}\{^1\text{H}\}$: δ 34.4 (br s), 15.7 (m). ^{19}F : δ -360.7 (br s). $^{13}\text{C}\{^1\text{H}\}$: δ 218.3 (br d, $J_{\text{CP}} = 93$ Hz, NCN), 204.0 (br d, $J_{\text{CF}} = 70$ Hz, Ru-CO). IR (C₆D₆, cm⁻¹): 1902 (ν_{CO}).

Ru(SIPr)(PPh₃)(CO)HF (6). A toluene (20 mL) solution of Ru(PPh₃)₃(CO)HF (100 mg, 0.1 mmol) was heated with SIPr(C₆F₅)H (160 mg, 0.29 mmol) in an ampule fitted with a PTFE tap at 393 K for 16 h. NMR spectroscopy showed full conversion to **6**. An alternative route involved addition of Et₃N·3HF (10 mg, 0.06 mmol) to a solution of Ru(SIPr)(PPh₃)₂(CO)H₂ (50 mg, 0.05 mmol) in benzene (10 mL). The solution was agitated at ambient temperature for 1 h before addition of CsF (40 mg, 0.29 mmol) and filtration by cannula. The solution was then reduced in *vacuo*,

redissolved in a minimum of C₆D₆, and transferred to a J. Youngs resealable NMR tube for characterization. ^1H NMR (C₆D₆, 500 MHz, 298 K):* δ 3.83 (sept, $J_{\text{HH}} = 6.72$ Hz, 2H, CH(CH₃)₂), 3.66 (s, 4H, NCH₂), 3.57 (sept, $J_{\text{HH}} = 6.72$ Hz, 2H, CH(CH₃)₂), 1.61 (d, $J_{\text{HH}} = 6.72$ Hz, 6H, CH(CH₃)₂), 1.40 (d, $J_{\text{HH}} = 6.72$ Hz, 6H, CH(CH₃)₂), 1.24 (d, $J_{\text{HH}} = 6.72$ Hz, 6H, CH(CH₃)₂), 1.18 (d, $J_{\text{HH}} = 6.72$ Hz, 6H, CH(CH₃)₂), -23.05 (d, $J_{\text{HP}} = 23.80$ Hz, 1H, Ru-H). *The presence of free PPh₃ prevented assignment of the aromatic region of the ^1H spectrum. $^{31}\text{P}\{^1\text{H}\}$: δ 38.3 (d, $J_{\text{PF}} = 26.1$ Hz). ^{19}F : δ -217.1 (br d, $J_{\text{FP}} = 24.8$ Hz). $^{13}\text{C}\{^1\text{H}\}$: δ 219.9 (d, $J_{\text{CP}} = 97.6$ Hz, NCN), 204.9 (br d, $J_{\text{CF}} = 75.8$ Hz, Ru-CO), 149.0 (s, C₆Pr₂H₃), 149.2 (s, C₆Pr₂H₃) 137.4 (N-C_{ipso}), 125.3 (s, C₆Pr₂H₃), 125.2 (s, C₆Pr₂H₃), 54.6 (s, NCH₂), 54.5 (s, NCH₂), 29.7 (s, CH(CH₃)₂), 29.5 (s, CH(CH₃)₂), 27.3 (s, CH(CH₃)₂), 27.1 (s, CH(CH₃)₂), 24.9 (s, CH(CH₃)₂), 24.7 (s, CH(CH₃)₂). IR (C₆D₆, cm⁻¹): 1922 (ν_{CO} , **6**), 1907 (ν_{CO} , **9**).

Ru(SIPr)(PPh₃)₂(CO)HF (9). In the presence of a total of 2.6 equiv of PPh₃ (5 mg, 0.019 mmol mmol), a solution of **6** (6 mg, 0.007 mmol) was transformed into a 50:50 mixture of **6** and Ru(SIPr)(PPh₃)₂(CO)HF (**9**) as shown by low temperature NMR spectroscopy. Selected NMR data. ^1H (400 MHz, C₆D₅CD₃, 201 K): δ -5.71 (dd, $J_{\text{HP}} = 121.45$, $J_{\text{HP}} = 24.91$ Hz, Ru-H). $^{31}\text{P}\{^1\text{H}\}$: δ 30.8 (m), 15.5 (m). ^{19}F : δ -367.0 (br s). IR (C₆D₆, cm⁻¹): 1907 (ν_{CO}).

Ru(IPr)(PPh₃)(CO)HF (7). A toluene (20 mL) solution of Ru(PPh₃)₃(CO)HF (100 mg, 0.10 mmol) was heated with IPr (110 mg, 0.29 mmol) at 363 K for 6 h to give 100% conversion to **7** by NMR spectroscopy. An alternative route to the complex involved the reaction of Ru(IPr)(PPh₃)₂(CO)H₂ (50 mg, 0.05 mmol) with Et₃N·3HF (10 mg, 0.06 mmol) in benzene (10 mL) at ambient temperature for 1 h, followed by addition of CsF (40 mg, 0.29 mmol), continued stirring at room temperature for 1 h, and finally filtration by cannula. The filtrate was reduced to dryness, redissolved in a minimum amount of C₆D₆, and transferred to a J. Youngs NMR tube for spectroscopic analysis. ^1H NMR (C₆D₆, 500 MHz, 298 K):* δ 6.62 (s, 2H, NCH), 3.30 (sept, $J_{\text{HH}} = 6.86$ Hz, 2H, CH(CH₃)₂), 3.10 (sept, $J_{\text{HH}} = 6.66$ Hz, 2H, CH(CH₃)₂), 1.54 (d, $J_{\text{HH}} = 6.66$ Hz, 6H, CH(CH₃)₂), 1.28 (d, $J_{\text{HH}} = 6.66$ Hz, 6H, CH(CH₃)₂), 1.12 (d, $J_{\text{HH}} = 6.86$ Hz, 6H, CH(CH₃)₂), 1.08 (d, $J_{\text{HH}} = 6.86$ Hz, 6H, CH(CH₃)₂), -22.83 (d, $J_{\text{HP}} = 23.78$ Hz, 1H, Ru-H). *The presence of free PPh₃ prevented assignment of the aromatic region of the ^1H spectrum. $^{31}\text{P}\{^1\text{H}\}$: δ 40.0 (d, $J_{\text{PF}} = 26.9$ Hz). ^{19}F : δ -209.9 (br s). $^{13}\text{C}\{^1\text{H}\}$: δ 205.3 (dd, $J_{\text{CF}} = 75.6$, $J_{\text{CP}} = 11.0$ Hz, Ru-CO), 194.7 (d, $J_{\text{CP}} = 104.1$ Hz, NCN), 148.0 (s, C₆Pr₂H₃), 147.8 (s, C₆Pr₂H₃), 137.2 (N-C_{ipso}), 124.7 (s, C₆Pr₂H₃), 124.6 (s, C₆Pr₂H₃), 124.2 (s, NCH), 29.7 (s, CH(CH₃)₂), 29.6 (s, CH(CH₃)₂), 27.0 (s, CH(CH₃)₂), 26.7 (s, CH(CH₃)₂), 24.0 (s, CH(CH₃)₂), 23.8 (s, CH(CH₃)₂). IR (C₆D₆, cm⁻¹): 1919 (ν_{CO} , **7**), 1906 (ν_{CO} , **10**).

Ru(IPr)(PPh₃)₂(CO)HF (10). In the presence of a total of 2.6 equiv of PPh₃ (5 mg, 0.020 mmol), low temperature NMR revealed complete conversion of **7** (6 mg, 0.008 mmol) to **10**. ^1H (C₆D₅CD₃, 400 MHz, 201 K): δ 6.68 (s, 1H, NCH), 6.67 (s, 1H, NCH) 4.06 (m, 1H, CH(CH₃)₂), 3.74 (m, 1H, CH(CH₃)₂), 3.56 (m, 1H, CH(CH₃)₂), 2.86 (m, 1H, CH(CH₃)₂), 1.80 (br m, 3H, CH(CH₃)₂), 1.62 (br m, 3H, CH(CH₃)₂), 1.24 (br m, 3H, CH(CH₃)₂), 1.18 (br m, 9H, CH(CH₃)₂), 0.97 (br m, 3H, CH(CH₃)₂), -0.17 (br m, 3H, CH(CH₃)₂), -5.53 (dd, $J_{\text{HP}} = 124.48$, $J_{\text{HP}} = 25.97$ Hz, 1H, Ru-H).

*The presence of free PPh₃ prevented assignment of the aromatic region of the ^1H spectrum. $^{31}\text{P}\{^1\text{H}\}$: δ 32.8 (m), 14.9 (m). ^{19}F : δ -369.1 (br s). IR (C₆D₆, cm⁻¹): 1905 (ν_{CO}).

Ru(IMes)(PPh₃)(CO)HF (11). Ru(IMes)(PPh₃)₂(CO)H₂ (50 mg, 0.05 mmol) was dissolved in benzene (10 mL) and Et₃N·3HF (13 mg, 0.08 mmol) added via syringe. The solution was agitated at ambient temperature for 1 h before addition of CsF (40 mg, 0.23 mmol) and filtration by cannula. The solution was then reduced to dryness, redissolved in a minimum amount of C₆D₆, and transferred to a J. Youngs NMR tube for analysis. ^1H NMR (C₆D₆, 500 MHz, 298 K):* δ 6.82 (s, 2H, C₆Me₃H₂), 6.75 (s, 2H, C₆Me₃H₂), 6.23 (s,

(69) Ahmad, N.; Levison, J. J.; Robinson, S. D.; Uttley, M. F. *Inorg. Synth.* **1974**, *15*, 45–64.

(70) Arduengo, A. J., III.; Krafczyk, R.; Schmutzler, R.; Craig, H. A.; Goerlich, J. R.; Marshall, W. J.; Unverzagt, M. *Tetrahedron* **1999**, *55*, 14523–14534.

(71) Jafarpour, L.; Stevens, E. D.; Nolan, S. P. *J. Organomet. Chem.* **2000**, *606*, 49–54.

(72) Nyce, G. W.; Csihony, S.; Waymouth, R. M.; Hedrick, J. L. *Chem.—Eur. J.* **2004**, *10*, 4073–4079.

(73) Bedford, R. B.; Betham, M.; Blake, M. E.; Frost, R. M.; Horton, P. N.; Hursthouse, M. B.; López-Nicolás, R.-M. *Dalton Trans.* **2005**, 2774–2779.

2H, NCH), 2.46 (s, 6H, CH₃), 2.31 (s, 6H, CH₃), 2.10 (s, 6H, CH₃), -23.10 (br s, 1H, Ru-H). ³¹P{¹H}: δ 39.5 (br d, *J*_{PH} = 24.6 Hz). ¹⁹F: δ -207.5 (br s). *The presence of free PPh₃ prevented assignment of the aromatic region of the ¹H spectrum. ¹³C{¹H}: δ 205.5 (dd, *J*_{CF} = 74.0, *J*_{CP} = 12.7 Hz, Ru-CO), 191.4 (d, *J*_{CP} = 103.9 Hz, NCN), 139.0 (s, CCH₃), 137.6 (s, CCH₃), 137.5 (s, N-C), 137.4 (s, CCH₃), 129.9 (s, *o*-*p*-C₆Me₃H₂), 129.8 (s, *o*-*p*-C₆Me₃H₂), 122.9 (s, NCH), 21.9 (s, CH₃), 19.2 (s, CH₃), 19.1 (s, CH₃). IR (C₆D₆, cm⁻¹): 1913 (ν_{CO}, 11), 1903 (ν_{CO}, 12).

Ru(IMes)(PPh₃)₂(CO)HF (12). In the presence of a total of 2.6 equiv of PPh₃ (8 mg, 0.029 mmol), a solution of **11** (7 mg, 0.010 mmol) was found by low temperature NMR spectroscopy to have undergone complete conversion to **12**. ¹H NMR (C₆D₅CD₃, 400 MHz, 201 K): δ 6.00 (s, 1H, NCH), 5.85 (s, 1H, NCH), 2.70 (s, 3H, CH₃), 2.54 (s, 3H, CH₃), 2.32 (s, 3H, CH₃), 2.24 (s, 3H, CH₃), 2.12 (s, 3H, CH₃), 1.35 (s, 3H, CH₃), -5.54 (dd, *J*_{HP} = 123.47, *J*_{HH} = 28.01 Hz, 1H, Ru-H). *The presence of free PPh₃ prevented assignment of the aromatic region of the ¹H spectrum. ³¹P{¹H}: δ 35.5 (m), 14.3 (m). ¹⁹F: δ -362.1 (br s). IR (C₆D₆, cm⁻¹): 1902 (ν_{CO}).

Ru(SIMes)(PPh₃)₂(CO)H₂ (13). Ru(PPh₃)₃(CO)HF (300 mg, 0.032 mmol) and SIMes(C₆F₅)H (450 mg, 0.096 mmol) were combined in an ampule fitted with a PTFE tap, dissolved in benzene (30 mL), and heated at 343 K for 2.5 h. The solution was filtered by cannula, Et₃SiH (0.25 mL, 0.157 mmol) was added to the filtrate, and the resulting solution was stirred at room temperature for 1 h. The resulting solution was reduced in volume, and EtOH (30 mL) was added with stirring to afford a red suspension of a white solid. The solid was isolated by cannula filtration, washed with hexane (2 × 30 mL), and dried under vacuum to give 152 mg of product (Yield: 49%). Analysis for C₅₈H₅₈N₂O₂P₂Ru [found (calculated)]: C, 72.41 (72.15); H, 6.08 (6.48); N, 2.91 (2.65). ¹H NMR (C₆D₆, 500 MHz, 298 K): 7.50–7.27 (m, 12H, PC₆H₅), 7.05–6.97 (m, 20H, PC₆H₅ + C₆Me₃H₂), 6.84 (br s, 2H, C₆Me₃H₂), 3.27 (br s, 4H NCH₂), 2.61 (br s, 3H, CH₃), 2.34 (s, 6H, CH₃), 2.21 (br s, 6H, CH₃), 1.51 (br s, 3H, CH₃), -6.63 (ddd, *J*_{HP} = 24.39, *J*_{HP} = 22.81, *J*_{HH} = 5.63 Hz, 1H, Ru-H), -8.20 (ddd, *J*_{HP} = 77.41, *J*_{HP} = 33.28, *J*_{HH} = 5.63 Hz, 1H, Ru-H). ³¹P{¹H}: δ 57.4 (d, *J*_{PP} = 15.8 Hz), 47.6 (d, *J*_{PP} = 15.8 Hz). ¹³C{¹H}: δ 224.9 (dd, *J*_{CP} = 72.1, *J*_{CP} = 6.5 Hz, NCN), 205.7 (dd, *J*_{CP} = 8.7, *J*_{CP} = 8.5 Hz, Ru-CO), 142.6 (d, *J*_{CP} = 13.7 Hz, PC₆H₅), 142.2 (s, NC_{ipso}), 138.8 (s, C₆Me₃H₂), 138.7 (d, *J*_{CP} = 13.7 Hz, PC₆H₅), 135.2 (s, C₆Me₃H₂), 135.3 (d, *J*_{CP} = 3.1 Hz, PC₆H₅), 133.1 (d, *J*_{CP} = 9.6 Hz, PC₆H₅), 132.1 (d, *J*_{CP} = 2.9 Hz, PC₆H₅), 131.8 (s, C₆Me₃H₂), 129.5 (d, *J*_{CP} = 2.0 Hz, PC₆H₅), 128.1 (d, *J*_{CP} = 8.6 Hz, PC₆H₅), 127.8 (d, *J*_{CP} = 9.0 Hz, PC₆H₅), 51.8 (s, NCH₂), 21.8 (CH₃). IR (nujol, cm⁻¹): 1941 (ν_{CO}).

Ru(SIPr)(PPh₃)₂(CO)H₂ (14). Ru(PPh₃)₃(CO)HF (130 mg, 0.14 mmol) and SIPr(C₆F₅)H (230 mg, 0.41 mmol) were dissolved in toluene (20 mL) in an ampule fitted with a PTFE tap, and the solution was refluxed at 393 K for 16 h. The reaction mixture was subsequently reduced to dryness, and hexane (20 mL) was added. The solution was subjected to cannula filtration, and Et₃SiH (0.10 mL, 0.63 mmol) was added to the filtrate. After stirring for 1 h at room temperature, the mixture was filtered and the light green solid was washed with EtOH (20 mL) and hexane (20 mL). Upon drying, Ru(SIPr)(PPh₃)₂(CO)H₂ was isolated as a white solid. Yield 39 mg (27%). Analysis for C₆₄H₇₀N₂O₂P₂Ru [found (calculated)]: C, 73.47 (73.16); H, 6.73 (6.97); N, 2.68 (2.47). ¹H NMR (C₆D₆, 500 MHz, 298 K): δ 7.80 (m, 2H, PC₆H₅), 7.46–7.20 (m, 13H, PC₆H₅ + C₆ⁱPr₂H₃), 7.13–7.00 (m, 4H, PC₆H₅ + C₆ⁱPr₂H₃), 6.99–6.78 (m, 13H, PC₆H₅ + C₆ⁱPr₂H₃), 6.72 (m, 2H, PC₆H₅), 6.61 (m, 2H, PC₆H₅), 4.00 (sept, *J*_{HH} = 6.73 Hz, 1H, CH(CH₃)₂), 3.95–3.64 (m, 6H, CH(CH₃)₂ + NCH₂), 2.99 (sept, *J*_{HH} = 6.73 Hz, 1H, CH(CH₃)₂), 1.72 (d, *J*_{HH} = 6.73 Hz, 3H, CH₃), 1.26 (d, *J*_{HH} = 6.73 Hz, 3H, CH₃), 1.21 (d, *J*_{HH} = 6.73 Hz, 3H, CH₃), 1.17 (d, *J*_{HH} = 6.73 Hz, 3H, CH₃), 1.15 (d, *J*_{HH} = 6.73 Hz, 3H, CH₃), 0.97 (d, *J*_{HH} = 6.73 Hz, 3H, CH₃), 0.69 (d, *J*_{HH} = 6.73 Hz, 3H, CH₃), 0.32 (d, *J*_{HH} = 6.73 Hz, 3H, CH₃), -6.47 (ddd, *J*_{HP} = 25.43, *J*_{HP} = 20.36, *J*_{HH} = 4.80 Hz, 1H, Ru-H), -8.40 (ddd, *J*_{HP} = 77.20, *J*_{HP} = 32.27, *J*_{HH}

= 4.80 Hz, 1H, Ru-H). ³¹P{¹H}: δ 55.2 (d, *J*_{PP} = 16.0 Hz), 44.5 (d, *J*_{PP} = 16.0 Hz). ¹³C{¹H}: δ 231.3 (dd, *J*_{CP} = 72.2, *J*_{CP} = 5.9 Hz, NCN), 205.7 (dd, *J*_{CP} = 8.6, *J*_{CP} = 7.9 Hz, Ru-CO), 149.2 (s, *o*-C₆ⁱPr₂H₃), 148.6 (s, *o*-C₆ⁱPr₂H₃), 148.5 (s, *o*-C₆ⁱPr₂H₃), 148.2 (s, *o*-C₆ⁱPr₂H₃), 143.9 (s, N-C), 141.7 (s, N-C), 141.6 (d, *J*_{CP} = 24.3 Hz, PC₆H₅), 139.5 (d, *J*_{CP} = 31.4 Hz, PC₆H₅), 136.4 (d, *J*_{CP} = 12.7 Hz, PC₆H₅), 136.4 (d, *J*_{CP} = 11.3 Hz, PC₆H₅), 135.3 (d, *J*_{CP} = 11.1 Hz, PC₆H₅), 134.6 (d, *J*_{CP} = 11.9 Hz, PC₆H₅), 129.8 (d, *J*_{CP} = 11.9 Hz, PC₆H₅), 128.2 (d, *J*_{CP} = 8.9 Hz, PC₆H₅), 127.9 (d, *J*_{CP} = 8.5 Hz, PC₆H₅), 127.5 (d, *J*_{CP} = 9.0 Hz, PC₆H₅), 126.1 (s, C₆ⁱPr₂H₃), 125.8 (s, C₆ⁱPr₂H₃), 125.6 (s, C₆ⁱPr₂H₃), 125.1 (s, C₆ⁱPr₂H₃), 55.5 (s, NCH₂), 54.5 (s, NCH₂), 30.0 (s, CH(CH₃)₂), 29.9 (s, CH(CH₃)₂), 29.6 (s, CH(CH₃)₂), 29.5 (s, CH(CH₃)₂), 27.6 (s, CH₃), 27.3 (s, CH₃), 27.2 (s, CH₃), 27.0 (s, CH₃), 25.4 (s, CH₃), 24.3 (s, CH₃), 24.1 (s, CH₃), 23.4 (s, CH₃). IR (nujol, cm⁻¹): 1953 (ν_{CO}).

Ru(IPr)(PPh₃)₂(CO)H₂ (15). Ru(PPh₃)₃(CO)HF (400 mg, 0.43 mmol) and IPr (250 mg, 0.64 mmol) were dissolved in toluene (30 mL) in an ampule fitted with a PTFE valve. The reaction mixture was heated at 363 K for 6 h, cooled to room temperature, and then concentrated. Hexane was added to the yellow solid, and the solution was filtered through a filter cannula. Et₃SiH (0.3 mL, 1.88 mmol) was added to the filtrate, which was then stirred for 1 h to afford a white precipitate. The mixture was filtered, and the solid was washed with EtOH (20 mL) and hexane (20 mL) and dried under vacuum to give Ru(IPr)(PPh₃)₂(CO)H₂ as a white powder. Yield 140 mg (31%). Analysis for C₆₄H₆₈N₂O₂P₂Ru [found (calculated)]: C, 73.61 (73.22); H, 6.56 (6.87); N, 2.68 (2.53). ¹H NMR (C₆D₆, 500 MHz, 298 K): δ 7.66–7.29 (m, 11H, PC₆H₅), 7.29–7.19 (m, 4H, C₆ⁱPr₂H₃), 7.14–7.07 (m, 2H, C₆ⁱPr₂H₃), 7.06–6.83 (m, 16H, PC₆H₅), 6.81 (d, *J*_{HH} = 1.78 Hz, 1H, NCH), 6.77 (d, *J*_{HH} = 1.78 Hz, 1H, NCH), 6.76–6.58 (br m, 3H, PC₆H₅), 3.50 (sept, *J*_{HH} = 6.80 Hz, 1H, CH(CH₃)₂), 3.44 (sept, *J*_{HH} = 6.80 Hz, 1H, CH(CH₃)₂), 3.37 (sept, *J*_{HH} = 6.80 Hz, 1H, CH(CH₃)₂), 2.95 (sept, *J*_{HH} = 6.80 Hz, 1H, CH(CH₃)₂), 1.66 (d, *J*_{HH} = 6.80 Hz, 3H, CH₃), 1.14 (d, *J*_{HH} = 6.80 Hz, 3H, CH₃), 1.10 (d, *J*_{HH} = 6.80 Hz, 3H, CH₃), 1.04 (d, *J*_{HH} = 6.80 Hz, 3H, CH₃), 1.02 (d, *J*_{HH} = 6.80 Hz, 3H, CH₃), 0.96 (d, *J*_{HH} = 6.80 Hz, 3H, CH₃), 0.80 (d, *J*_{HH} = 6.80 Hz, 3H, CH₃), 0.25 (d, *J*_{HH} = 6.80 Hz, 3H, CH₃), -6.27 (dt, *J*_{HP} = 23.65, *J*_{HP} = 23.59, *J*_{HH} = 5.60 Hz, 1H, Ru-H), -8.14 (ddd, *J*_{HP} = 82.85, *J*_{HP} = 31.16, *J*_{HH} = 5.60 Hz, 1H, Ru-H). ³¹P{¹H}: δ 44.6 (d, *J*_{PP} = 13.7 Hz), 57.6 (d, *J*_{PP} = 13.7 Hz). ¹³C{¹H}: δ 205.6 (dd, *J*_{CP} = 8.7, *J*_{CP} = 8.4 Hz, Ru-CO), 202.8 (dd, *J*_{CP} = 75.8, *J*_{CP} = 7.6 Hz, NCN), 149.1 (s, *o*-C₆ⁱPr₂H₃), 149.0 (s, *o*-C₆ⁱPr₂H₃), 146.8 (s, *o*-C₆ⁱPr₂H₃), 146.5 (s, *o*-C₆ⁱPr₂H₃), 141.9 (d, *J*_{CP} = 36.1 Hz, PC₆H₅), 142.2 (d, *J*_{CP} = 36.4 Hz, PC₆H₅), 140.1 (s, N-C), 135.3 (d, *J*_{CP} = 11.5 Hz, PC₆H₅), 130.7 (s, PC₆H₅), 129.6 (s, PC₆H₅), 129.0 (s, PC₆H₅), 128.6 (s, PC₆H₅), 127.9 (d, *J*_{CP} = 9.4 Hz, PC₆H₅), 126.3 (s, C₆ⁱPr₂H₃), 125.6 (s, NCH), 125.6 (s, C₆ⁱPr₂H₃), 125.3 (s, C₆ⁱPr₂H₃), 125.2 (s, C₆ⁱPr₂H₃), 125.2 (s, C₆ⁱPr₂H₃), 125.1 (s, C₆ⁱPr₂H₃), 125.1 (s, NCH), 30.3 (s, CH(CH₃)₂), 29.8 (s, CH(CH₃)₂), 29.6 (s, CH(CH₃)₂), 29.5 (s, CH(CH₃)₂), 27.1 (s, CH₃), 26.9 (s, CH₃), 26.8 (s, CH₃), 26.7 (s, CH₃), 24.3 (s, CH₃), 23.6 (s, CH₃), 22.9 (s, CH₃), 22.8 (s, CH₃). IR (nujol, cm⁻¹): 1947 (ν_{CO}). ESI-TOF MS: [M-PPh₃-H₂+H]⁺ *m/z* = 781.2882 (theoretical *m/z* = 781.2868).

Kinetic Experiments. A THF solution of **15** (0.01 M), fluoroarene (0.1 M), Et₃SiH (0.1 M), and α,α,α-trifluorotoluene (0.08 M) as standard were added to an NMR tube fitted with a J. Youngs resealable valve in the glovebox. The tube was placed into the preheated (339 K) probe of a 400 MHz NMR spectrometer, and ¹⁹F spectra were recorded periodically for a total of 12 h (relaxation times of 20 s were employed to ensure correct integrations).⁷⁴

HDF Experiments for Determination of Turnover Numbers.

An NMR tube fitted with a J. Youngs resealable valve was loaded with a ruthenium complex (0.01 M), fluoroarene (0.1 M), and alkylsilane (0.2 M) in THF, benzene, or toluene in the glovebox, and a standardized capillary tube of α,α,α-trifluorotoluene was inserted. An initial ¹⁹F spectrum was recorded at room temperature, the capillary was removed from the NMR tube, and the

Table 5. Data Collection and Refinement Details for Compounds **5**, **11**, **13**, **14**, and **15**

compound	5	11	13	14	15
empirical formula	C ₄₀ H ₄₂ FN ₂ OPRu	C ₄₄ H ₄₈ FN ₂ O ₂ PRu	C ₅₈ H ₅₈ N ₂ OP ₂ Ru	C ₆₈ H ₇₈ N ₂ O ₂ P ₂ Ru	C ₆₈ H ₇₆ N ₂ O ₂ P ₂ Ru
formula weight	717.80	787.88	962.07	1118.33	1116.32
<i>T</i> /K	150(2)	150(2)	150(2)	150(2)	150(2)
crystal system	monoclinic	monoclinic	triclinic	orthorhombic	orthorhombic
space group	<i>P</i> 2 ₁ / <i>a</i>	<i>P</i> 2 ₁ / <i>a</i>	<i>P</i> 1	<i>P</i> 2 ₁ <i>cn</i>	<i>P</i> 2 ₁ <i>cn</i>
<i>a</i> /Å	15.1040(2)	13.7310(1)	11.3050(2)	11.7530(1)	11.6010(1)
<i>b</i> /Å	14.1360(2)	13.6060(1)	11.8970(3)	12.4800(1)	12.6060(2)
<i>c</i> /Å	16.7450(3)	21.7640(3)	20.7740(6)	39.0720(4)	39.3500(6)
α /deg	90	90	96.212(1)	90	90
β /deg	99.633(1)	105.746(4)	96.477(1)	90	90
γ /deg	90	90	118.000(2)	90	90
<i>U</i> /Å ³	3524.82(9)	3913.46(7)	2409.50(10)	5730.98(9)	5754.63(14)
<i>Z</i>	4	4	2	4	4
<i>D</i> /g cm ⁻³	1.353	1.337	1.326	1.296	1.288
μ /mm ⁻¹	0.529	0.485	0.435	0.377	0.375
<i>F</i> (000)	1488	1640	1004	2360	2352
crystal size/mm ³	0.25 × 0.20 × 0.12	0.25 × 0.25 × 0.10	0.25 × 0.13 × 0.10	0.15 × 0.07 × 0.07	0.15 × 0.07 × 0.07
θ min., max for data collection	3.70, 27.47	4.77, 30.04	3.62, 27.45	3.53, 27.45	3.52, 25.00
index ranges	-18 ≤ <i>h</i> ≤ 19; -18 ≤ <i>k</i> ≤ 18; -21 ≤ <i>l</i> ≤ 21	-19 ≤ <i>h</i> ≤ 19; -19 ≤ <i>k</i> ≤ 19; -30 ≤ <i>l</i> ≤ 30	-14 ≤ <i>h</i> ≤ 14; -15 ≤ <i>k</i> ≤ 15; -25 ≤ <i>l</i> ≤ 26	-15 ≤ <i>h</i> ≤ 15; -16 ≤ <i>k</i> ≤ 16; -50 ≤ <i>l</i> ≤ 50	-13 ≤ <i>h</i> ≤ 13; -14 ≤ <i>k</i> ≤ 14; -45 ≤ <i>l</i> ≤ 46
reflections collected	56 161	79 321	24 476	83 489	60 542
independent reflections, <i>R</i> _{int}	8060, 0.0564	11 386, 0.0600	10 596, 0.0441	12 837, 0.0933	10 099, 0.0914
reflections observed (>2 σ)	6642	8514	8742	9950	7990
data completeness	0.996	0.993	0.961	0.997	0.996
absorption correction	multiscan	multiscan	multiscan	multiscan	multiscan
max., min. transmission	0.94, 0.89	0.95, 0.89	0.96, 0.92	0.97, 0.92	0.96, 0.93
data/restraints/parameters	8060/2/430	11 386/3/493	10 596/2/601	12 837/30/711	10 099/15/689
goodness-of-fit on <i>F</i> ²	1.071	1.054	1.146	1.048	1.062
final <i>R</i> 1, <i>wR</i> 2 [<i>I</i> > 2 σ (<i>I</i>)]	0.0318, 0.0729	0.0396, 0.0945	0.0504, 0.1100	0.0472, 0.0757	0.0470, 0.0792
final <i>R</i> 1, <i>wR</i> 2 (all data)	0.0443, 0.0787	0.0646, 0.1059	0.0670, 0.1168	0.0778, 0.0843	0.0730, 0.0874
largest diff. peak, hole/eÅ ⁻³	0.677, -0.547	0.741, -0.561	0.961, -0.845	0.521, -0.508	0.528, -0.461
Flack parameter	-	-	-	0.01(2)	-0.03(3)

reaction mixture was then heated in an oil bath at 343 K for a set period of time. The NMR tube was removed from the oil bath and cooled, and the capillary was reinserted before further ¹⁹F spectra⁷⁴ were periodically recorded. HDF products were integrated relative to the standard and identified by comparison to authentic samples purchased from Fluorochem, Aldrich, or Apollo Scientific.

X-ray Crystallography. Single crystals of compounds **5**, **11**, **13**, **14**, and **15** were analyzed using a Nonius Kappa CCD diffractometer. Details of the data collections, solutions, and refinements are given in Table 5. The structures were solved using SHELXS-97⁷⁵ and refined using full-matrix least-squares in SHELXL-97.⁷⁵ Where hydrides were located, they were universally refined at a distance of 1.6 Å from the central metal. Refinements were generally straightforward. Nonetheless, the following points are noteworthy. In **5**, the hydride was located and modeled over two positions in 50:50 ratio, based on maxima in the penultimate difference Fourier map. Carbonyl disorder in a 70:30 ratio evident in **11** necessarily means that the hydride must be similarly disordered. However, as the major hydride

component was readily located, it was refined at full occupancy (as there was no credible possibility of locating 0.3 of a hydrogen atom!). The asymmetric unit in this structure was also seen to contain one molecule of THF, also disordered over two sites in a similar ratio to that for the carbonyl. The minor component partial atoms in the solvent were treated isotropically in the final stages of refinement. C3 and C4 of the NHC ring in **13** were disordered in a 60:40 ratio over two sites. Analysis of **14** showed that one molecule of THF was also present in the asymmetric unit, in which two carbons were disordered in a 45:55 ratio. These disordered atomic fragment atoms were refined subject to distance and ADP restraints. A very small crystal was chosen for **15**, in order to ensure the sample was “single”. Consequently, data cutoff is at a Bragg angle of 25°. The asymmetric unit was seen to contain one molecule of THF in which the carbon atoms were disordered. This disorder was modeled over two sites in a 40:60 ratio, with O–C and C–C bond distances therein restrained to being similar.

Crystallographic data for compounds **5**, **11**, **13**, **14**, and **15** have been deposited with the Cambridge Crystallographic Data Centre as supplementary publications CCDC 697987–697991. Copies of the data can be obtained free of charge on application to CCDC, 12 Union Road, Cambridge CB2 1EZ, UK [fax: (+44) 1223 336033, e-mail: deposit@ccdc.cam.ac.uk].

(74) Kaspi, A. W.; Yahav-Levi, A.; Goldberg, I.; Vignalok, A. *Inorg. Chem.* **2008**, *47*, 5–7.

(75) Sheldrick, G. M. *Acta Crystallogr.* **1990**, *46*–47B, A46. Sheldrick, G. M. SHELXL-97, a computer program for crystal structure refinement, University of Göttingen, 1997.

Acknowledgment. We acknowledge Johnson Matthey plc for the loan of RuCl₃. Financial support was provided via a Doctoral Training Award to S.P.R. We thank Dr. John Lowe for help with NMR experiments, Profs. Stuart Macgregor and Robin Perutz for invaluable discussions, and Prof. Andrew Weller for the loan of high pressure NMR tubes.

Supporting Information Available: X-ray crystallographic files in CIF format for complexes **5**, **11**, **13**, **14**, and **15**. Analytical and structural data for Ru(NHC)₂(PPh₃)(CO)₂HF (**17–20**). This material is available free of charge via the Internet at <http://pubs.acs.org>.

JA806545E